in silico Plants, 2025, 7, diaf011
https://doi.org/10.1093/insilicoplants/diaf011
Advance access publication 16 July
Original Research

in silico Plants
OXFORD

Original Research

A functional–structural plant model for climbing bean: simulating light capture in maize/bean polycultures

Rik J. L. Rutjens[1,*], Jochem B. Evers[2], Leah R. Band[1,3], Matthew D. Jones[4], Markus R. Owen[1]

[1]School of Mathematical Sciences, University of Nottingham, University Park, Nottingham NG7 2RD, United Kingdom
[2]Centre for Crop Systems Analysis, Wageningen University & Research, Bornsesteeg 48, Wageningen 6708PE, The Netherlands
[3]Division of Plant and Crop Sciences, School of Biosciences, University of Nottingham, Sutton Bonington Campus, Loughborough LE12 5RD, United Kingdom
[4]School of Geography, University of Nottingham, University Park, Nottingham NG7 2RD, United Kingdom

[*]Corresponding author. Rik J. L. Rutjens, School of Mathematical Sciences, University of Nottingham, University Park, Nottingham NG7 2RD, United Kingdom.
E-mail: rik.rutjens@rmit.edu.au

Handling Editor: Dr. Xin-Guang Zhu

Abstract. A novel functional–structural plant (FSP) model for climbing common bean has been developed, encompassing twining behaviour and physical plant–plant interactions. The model enabled simulation of maize/bean polycultures, where common bean climbed upwards around the maize stalk, elucidating how plant architecture facilitates light capture in such polycultures. Employing sensitivity analysis, parameters have been identified that have the most influence on key outputs such as leaf area index and aboveground biomass. Simulations revealed limited maize growth impact but significant bean growth reduction in the polyculture compared to monocultures. Considering three different environmental conditions, the model suggested that the environment greatly affects model outputs in both the monocultures and polyculture, predicting that, within the polyculture, there would be very little bean growth in Dutch and French conditions. In contrast, the polyculture developed in Mexican conditions, with bean growth influenced by the magnitude of the time delay between maize and bean germination. Simulations in Mexican conditions predicted an increase in total peak biomass of up to 60%, in agreement with experimental observations of overyielding in polycultures. This indicates that aboveground processes (specifically light capture; in addition to root system complementarity) play an important role in the phenomenon of overyielding. In addition, it confirms that such agricultural systems may play a role in sustainable agricultural intensification. The maize/bean model presented in this work is one of the first examples of an aboveground FSP model of a polyculture with complex plant–plant interaction. Our results suggest that FSP modelling could be a valuable tool to investigate such agricultural systems.

Keywords: functional–structural plant model (FSPM); maize–bean polyculture

1. INTRODUCTION

The vast majority of cultivated land, ~80%, is grown in monoculture (Altieri and Nicholls 2020). This form of agriculture suffers from a host of issues: increased soil erosion, susceptibility to pathogens, and high dependency on inputs such as fertilizer, pesticides and irrigation (Altieri 1999, Gliessman 2014). On the other hand, there is a myriad of farming systems based around crop mixtures or intercrops (Altieri 1999), that exhibit many potential benefits over monocultures (Gliessman 2014). The focus in this work is on systems centring around maize (*Zea mays*) and common bean (*Phaseolus vulgaris*). Examples include intensive maize/bean intercrops (Béasse and Kouassi 2019, Fischer et al. 2020, Böhm et al. 2022, Carrel Strickhof), the three sisters (an intercrop of maize, bean and squash) (Pleasant 2016), and the milpa (López-Forment , 1998, Schmook et al. 2013, Maya Forest Gardeners - The Milpa n.d.), an ancient Maya Yucatex indigenous way of farming, on which millions of smallholder farmers still depend today. It has been shown in several field experiments that maize/bean polycultures can lead to higher yield and biomass compared to the crops grown in monoculture (a phenomenon called *overyielding*) (Tilman et al. 2001, Tsubo et al. 2003, Gliessman 2014). Postma and Lynch (2012) showed that this may at least partly be due to niche complementarity in the root system (e.g. different root architectures and different nutrient requirements and uptake rates). They demonstrated this using 3D functional–structural plant (FSP) modelling of root traits. Such work has been extended to the aboveground parts of the plant for other cereal/legume polycultures (maize/soybean

Li et al. 2021 and wheat/pea Barillot et al. 2014), but not maize/common bean polycultures.

In maize/bean polycultures a climbing variety of common bean is typically used, where the bean climbs upwards around the maize stalk. This leads to a complex architectural layout in both time and space. FSP models could be a useful tool for simulating such agricultural systems, as the explicit inclusion of plant architecture allows one to integrate these plant–plant interactions. However, no aboveground FSP model of climbing common bean exists, neither for monocultures (e.g. growing on poles) nor for maize/bean polycultures.

A detailed biomechanical description of twining or climbing is given by Moulton et al. (2020), who presented a complete multi-scale model for plant tropisms, from hormone distributions at the cell level to global stem deformation. With their model, they were able to simulate a wide range of plant tropisms, including climbing and twining behaviour. See also Isnard et al. (2009), Goriely and Neukirch (2006), and Fiorello et al. (2020) and the references therein for a broader background. However, describing bean twining and physical plant–plant interactions in an FSP model in such biomechanical detail is typically prohibited by two bottlenecks. First, the programming languages used to implement FSP models typically have limited suitability for complex numerical computations [e.g. solving (partial) differential equations]. The second bottleneck is computational expense. FSP models of plant stands typically operate at the organ scale and describe each plant in the stand and each organ of that plant individually (Sievänen et al. 2014). As such, processes like light capture, photosynthesis, resource allocation, and growth need to be calculated for potentially thousands to tens of thousands of organs. Adding a detailed biomechanical computation of the bean twining behaviour is likely to lead to unreasonable simulation times.

Efforts have also been made to model climbing plants with a focus on visual realism (e.g. for game design), without integrating biophysical mechanisms. Among these are FSP models for common ivy (Smolenova and Hemmerling 2008) and grape (Bahr et al. 2021), an L-system implementation for climbing plants (Knutzen 2009), and a procedural approach for modelling climbing plants with tendrils (Wong and Chen 2016) (see Greene 1989, Hädrich et al. 2017, Arvo and Kirk n.d., Benes and Míllá 2002) and the references therein for more information). However, most of these do not include twining behaviour. The ones that do (e.g. Wong and Chen 2016), often model the stem as a flexible string of particles (instead of a sequence of cylinders), where (biomechanical) rules on the particles determine the shape of the string (and thus the stem) (Greene 1989, Knutzen 2009, Arvo and Kirk n.d.). For collision detection, instead of ray-tracing or line-volume intersection, (i) space is often divided into many small cubes (voxels), and collisions are resolved at the voxels that are intersected by two or more objects (Wong and Chen 2016, Benes and Míllá 2002); or (ii) bounding volume hierarchies are used (Knutzen 2009, Wong and Chen 2016), where geometric objects are encased in a simpler bounding volume (e.g. a sphere or box), and collision detection is performed on those bounding volumes first; only those objects whose bounding volume intersects with another volume are then further investigated in detail. The way FSP models represent both stems and the external environment differs between modelling platforms. Therefore, here we develop an alternative approach for modelling twinning appropriate where stems are represented as a sequence of cylinders within continuous space (as is customary in GroIMP).

The objective of this study is two-fold: firstly, to develop an FSP model for (climbing) common bean with a focus on simplicity and plausible performance. Secondly, to investigate to what extent aboveground complementarity contributes to overyielding in maize/bean polycultures. As an example, differences in shoot and leaf architecture, such as the small bean leaves close to the maize stem versus the thin and long maize leaves pointing away from the maize stem, might enable common bean to fill the gaps between maize leaves, capturing light without hindering maize development. The hypothesis tested in this article is therefore the following: *Architectural facilitation in the bean/maize polyculture leads to enhanced light capture (hence improved biomass production) when compared to growing these crops in monoculture.* The focus will be on the aboveground process of light capture and subsequent carbon assimilation, leading to biomass increase. For modelling work on the belowground architecture in the three sisters, we refer to Postma and Lynch (2012).

Having described the model in Section 2, we first consider a stand of climbing bean twining around poles (Section 3). We perform global sensitivity analysis to evaluate the importance of model parameter values to key model outputs, including leaf area index, aboveground biomass and accumulated CO_2; this analysis identifies parameter values that have the most influence on these model outputs. Focusing on six of the important bean model parameters, we then simulate the full polyculture model of climbing bean with maize as its supporting medium (Section 4). We use the model to assess how the use of a polyculture (rather than a monoculture) affects the predicted plant architecture and biomass, and how these outputs are affected by model parameter values and environmental conditions.

2. MODEL DESCRIPTION

2.1 General model description

The model is a general modular FSP model using the platform GroIMP (Hemmerling et al. 2008). It simulates above ground plant growth and architectural development, driven by competition between plants for light and nutrients. It is an evolution of the model presented in Evers and Bastiaans (2016).

In this study, we simulate maize (*Z. mays*) and common bean (*P. vulgaris*) at a daily time step based on the principles of assimilate supply and demand. Plant organs serve either as a pure sink for assimilates (the generative organs and the roots), or both as a source and a sink depending on their age and surface area (the leaves and the stem segments). Bean is considered both in monoculture (growing on vertical poles) and in polyculture with maize, where it twines around the maize stalk.

2.1.1 Environment. To accurately represent a realistic light field, a mix of direct and diffuse light sources are placed in the scene. Seventy-two diffuse light sources are configured in

6 rings at different heights, and 24 direct light sources describe an arc in the sky to emulate the sun's path (Evers and Bastiaans 2016). The angle and orientation of the arc depend on the day of the year and latitude; the power of the light sources depends on the day of the year, the location in the sky, latitude, and transmissivity. The relative contribution of the diffuse and direct light sources is constant over a simulation, with the fraction of diffuse light of the total incoming radiation set to 0.8. Further details of the diffuse/direct radiation calculation can be found in Goudriaan and Van Laar (1994), Spitters et al. (1986), and Spitters (1986). At each time step, rays of photosynthetically active radiation (PAR) cast by the light sources are absorbed, reflected or transmitted by leaves and stems according to organ-independent optical coefficients, using the stochastic ray tracer capabilities of GroIMP (Hemmerling et al. 2008).

The average daily temperature follows one of three yearly patterns (Fig. 1). The Dutch climate (based on data from the Royal Dutch Meteorological Institute, 2001–19) is represented by a sinusoidal pattern over the year:

$$t_{\text{av}} = \text{tav}_a + \text{tav}_b \cdot \sin\left(\frac{2\pi(\text{DOY} - 111)}{365}\right), \quad (1)$$

where the minimum value is reached around Day 20, the mean at Day 111, and the maximum around Day 202. It is characterized by a mean value (tav_a) and the amplitude of the deviation around that mean (tav_b). $\text{DOY} \in \{1, 2, \ldots, 365\}$ denotes the day of the year. Secondly, a beta-distribution profile represents the temperature in the Yucatán peninsula in Mexico, given by World Bank (n.d.):

$$t_{\text{av}} = \text{tav}_a + \text{tav}_b \left(\frac{\text{DOY}}{365}\right)^{100/49} \left(1 - \frac{\text{DOY}}{365}\right)^4. \quad (2)$$

Finally, the following intermediate profile is also considered, which represents the yearly temperature in the Aquitaine region of (South-West) France (average summer temperatures, slightly warmer winters than the long-term average; polynomial fitted to data (1991–2020) from Météo-France n.d.):

$$\begin{aligned} t_{\text{av,FR}} = {} & 8.987 \cdot 10^{-11}\,\text{DOY}^5 - 7.350 \cdot 10^{-8}\,\text{DOY}^4 \\ & + 1.855 \cdot 10^{-5}\,\text{DOY}^3 - 1.621 \cdot 10^{-3}\,\text{DOY}^2 \\ & + 1.006 \cdot 10^{-1}\,\text{DOY} + 9.902. \end{aligned} \quad (3)$$

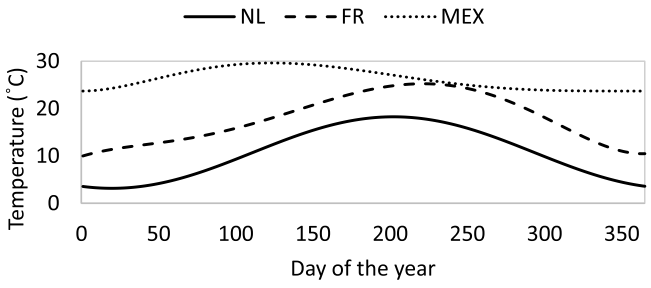

Fig. 1. Temperature profiles used in this work, representing the Netherlands (NL), the Aquitaine region in France (FR), and the Yucatán peninsula in Mexico (MEX).

Other atmospheric parameters such as CO_2 level, vapour pressure deficit, and O_2 level are kept constant throughout a simulation and are equal across environments. It should be noted that the formulas used for mean daily temperatures are mostly illustrative, aiming to create three distinct environmental scenarios. They are not necessarily complete descriptions of the current or *typical* climate in a particular location. In each location, the climate naturally varies each year, however considering such variations is beyond the scope of this study.

2.1.2 Physiology. At the organ level, the absorbed PAR is used to calculate photosynthesis rate as a function of organ nitrogen level (Evers and Bastiaans 2016). Assimilated CO_2 is converted into growth substrates, and maintenance costs are deducted. This leads to a daily pool of substrates available for organ growth.

Photosynthesis is described by the Farquhar–von Caemmerer–Berry (FvCB) model as in Yin and Struik (2009). The FvCB model implemented here predicts the net photosynthesis rate as a function of leaf nitrogen, absorbed light, and temperature, as the minimum of the Rubisco-limited and the electron transport-limited rates of CO_2 assimilation. The FvCB model is the standard in relating photosynthetic carbon assimilation to the concentration of intercellular CO_2 and absorbed photosynthetically active radiation (Dubois et al. 2007). For common bean the original C3 model is used, for maize a C4-equivalent is implemented (both described in Yin and Struik 2009).

Potential organ growth rate is defined as the organ demand for growth substrates (its sink strength), implemented using the first derivative of a beta growth function (Yin et al. 2003, Evers and Bastiaans 2016). To determine actual growth rate, the relative sink strength concept is used (Heuvelink 1996), in which the sink strength of an organ is expressed as a fraction of total plant sink strength. Depending on substrate availability and relative sink strength, organs grow at or below their potential rate. Any excess growth substrates (which may arise when all organs are growing at their potential rate) are made available for growth in the next time step.

Finally, organ size is updated based on the substrates received by each organ, using parameters for leaf mass per unit of leaf area (LMA) for the leaves, and specific internode length (SIL) for the internodes. Specifically for maize internodes, additional extension due to shade avoidance (Huber et al. 2021) is implemented by making SIL dependent on the level of competition experienced by the plant (Evers and Bastiaans 2016).

2.1.3 Plant development. Plant development is temperature driven, with a daily thermal time increment depending on the average daily temperature (see Section 2.1.1) and the species base temperature (tb). Subsequent leaves are initiated and appear at constant thermal time intervals (plastochron and phyllochron, respectively). For maize, which has a determinate growth habit (i.e. growth ceases during the natural lifespan of an individual), the total number of phytomers produced during a plant's lifespan is taken as constant and equal for all plants. If a leaf reaches a certain age or receives less light over a day than a given threshold, it will be shed.

2.1.4 Plant architecture. To mimic maize architecture, the first four internodes do not elongate, resulting in the corresponding

leaves emerging near the soil level. Leaves are represented by narrow oblong surfaces (see Evers and Bastiaans 2016). Consecutive leaves appear along the stem at a constant phyllotactic angle.

Common bean exhibits helix-like upwards growth around a climbing medium (pole or maize internode). The mean helix inclination (i.e. steepness) is constant and equal for all plants, but inclination for internodes with a phytomer rank larger than 1 is perturbed randomly (uniformly between -10° and 10°) to capture natural variation (based on Atala and Gianoli 2008; no specific data were found on climbing common bean). At each time step throughout a bud's lifetime, it may break with a fixed probability, resulting in a branch. In the model, internodes (represented by cylinders) of other plant species typically elongate over time. For a twining plant, since internode orientations do not change once they are initiated, lengthening leads to a worse (looser) fit of the helix, and potentially to collisions. Bean internode elongation is therefore set to zero, and new internodes are initiated with their final length. Thus, it is assumed that bean only experiences tip growth. Internode length varies according to

$$L = 0.03 + \frac{L_{\max} - 0.03}{\left(1 + 2e^{-(\text{rank}-1)}\right)^3}, \quad (4)$$

where rank denotes the phytomer rank of the internode, 0.03 m is the minimum internode length, and $L_{\max}$ is the maximum internode length, i.e. internodes that appear later are longer. The other constants in the denominator have been determined empirically, based on data in Durigon et al. (2019), Kelly (2001), and Kahlen and Stützel (2011).

Bean leaves are trifoliate, with the central petiolule being longer than the other two (×1.5), and the central leaflet being slightly wider (×1.5) and longer (×1.2) than the other leaflets. The side leaflets are inserted in the same plane as the central leaflet, but rotated 60° outwards. Leaves appear on the stem under such a phyllotactic angle that the petiole points outwards of the helix. Bean pods are included to accurately simulate light capture by leaves and are represented by pairs of grey rectangular boxes, the dimensions of which are determined by the pod weight. Pods only appear after 35 simulated days.

As the focus is on aboveground processes and interaction in this work, the root system architecture is not explicitly modelled for either species.

2.1.5 Model parameterization. Environmental parameters that are not location-specific (e.g. CO_2 level, vapour pressure deficit) and plant parameters for maize or those that are not species-specific (e.g. FvCB photosynthesis module parameters) are taken from previous work [as referenced throughout Section 2.1, particularly (Evers and Bastiaans 2016, Rutjens et al. 2024) and the references therein]. Some of these parameter values were derived in monoculture settings, or in different polycultures than maize/bean. Bean parameters are based on data in the literature wherever possible (as referenced throughout Section 2.1, and listed in Supplementary Material S5). However, for several parameters (e.g. specific internode length) no data were available, in which case a value was chosen based on values for other crops implemented in the GroIMP model (these parts of the model are not further used in this work and thus not described here). For several other parameters, data was only available for other bean species (not common bean), or common bean with different growth behaviours (e.g. bush bean; as highlighted in Supplementary Table S3).

2.2 A GroIMP model for climbing common bean

This section provides a concise overview of how the climbing behaviour of common bean is described in a GroIMP model. For a more extensive treatize the interested reader is referred to Supplementary Material S1. This is a proof of principle, and one of the first examples of (FSP) modelling intercrops with this level of complexity.

Bean climbing around a pole or maize stem is described by an approximate (discrete) helical trajectory (Supplementary Fig. S1), where the lengths of the discrete helix segments are given by the bean internode lengths. For simplicity, we ignore twining around noncylindrical objects such as leaves or flowers, and do not incorporate bean stems twining around themselves or other bean stems. We use global-to-local (and local-to-global) transformation matrices (Supplementary Material S1.2) and geometrical identities to specify transformations and rotations of the bean apex at each time step, which allow for easy control of the helix radius.

In short, given a climbing medium F (e.g. a pole or maize internode) and a bean apex A, bean growth consists of the following phases (Fig. 2):

(i) if A is too far from F, the bean grows towards F using a positional tropism (Section 2.2.1); this acts as a simple replacement for processes like circumnutation (circular movement of growing organs) and thigmotropism (organ movement upon physical touching);
(ii) if A is sufficiently close to F, the following steps are taken. First, A is given the correct orientation (Section 2.2.2). Subsequently the bean twines around F, describing a polygon in F's (x, y)-plane (Section 2.2.3) and moving in the z-direction with constant pitch. Whenever necessary (e.g. when changing from one climbing medium to the next, when encountering a collision (Section 2.2.4), or when taking a larger turn to grow closer to the climbing medium), A will be reoriented again on the next step to ensure the proper heading for the helix.

2.2.1 Growing towards a climbing medium. Mechanistically how a bean plant grows towards a pole is not well understood, and suitable macro-scale rules for prescribing such growth in an FSP model are not established. We suppose that the bean grows towards the pole as follows. The closest pole is found by looping over all poles in the scene, calculating the minimal Euclidean distance from the current apex to said pole, and subsequently selecting the one with the lowest distance (Supplementary Fig. S3). If this distance is larger than some predefined threshold, the bean grows towards the pole F using a positional tropism (i.e. a change in the head direction of apex a with a certain strength towards a specified point). This behaviour is a simple alternative for describing the more complex processes of circumnutation ('scouting' of the surrounding area) and thigmotropism (starting helical climbing behaviour upon finding a

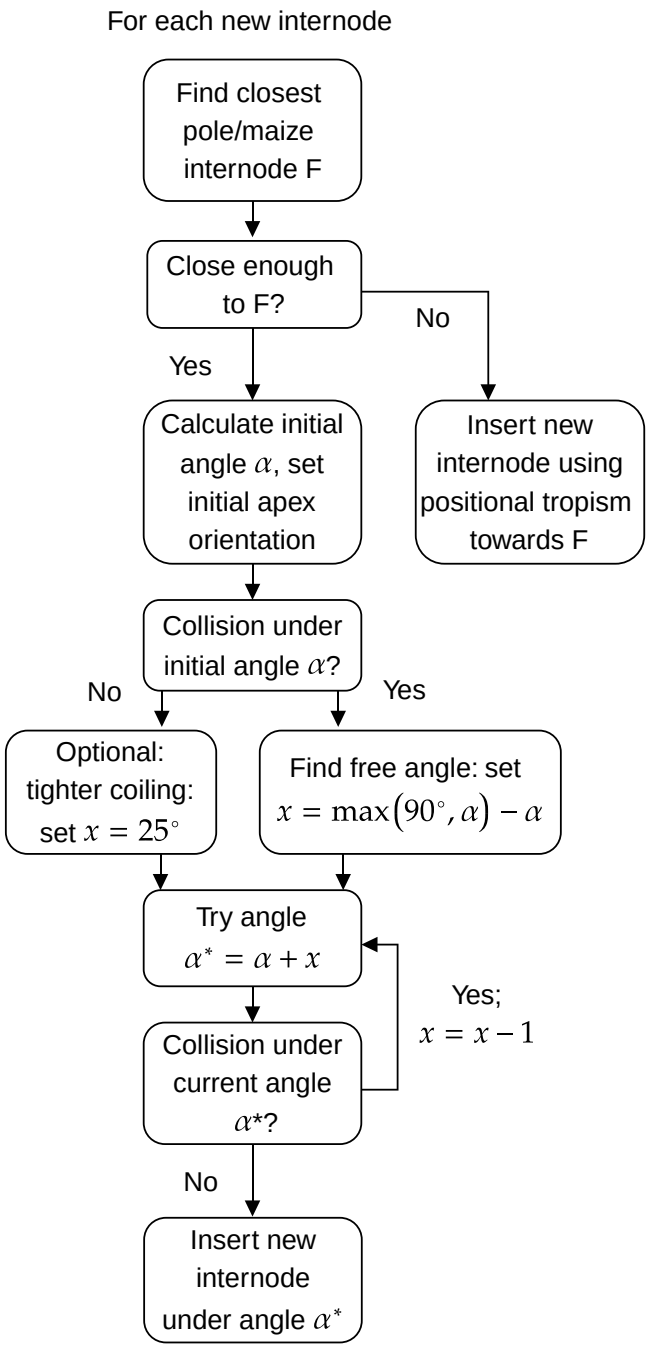

Fig. 2. Algorithm for inserting a new bean internode under the correct heading for twining around a pole or maize internode.

climbing medium). The point the tropism is directed towards is given (in global coordinates) by:

$$\begin{aligned} p_{\text{trop}} &= (F_x, F_y, F_z) \\ &\quad + \left(|A_z - F_z| \sin(\theta) + \zeta' \cos(\theta) + L \sin(\eta)\right) \text{dir}_F; \\ \zeta' &= \sqrt{(A_x - F_x)^2 + (A_y - F_y)^2}; \\ \theta &= \text{angle}(\text{dir}_F, \text{proj}(\text{dir}_F)). \end{aligned} \tag{5}$$

Here, (F_x, F_y, F_z) are the coordinates of the centrepoint of the bottom of F (Fig. 3), (A_x, A_y, A_z) are the global coordinates

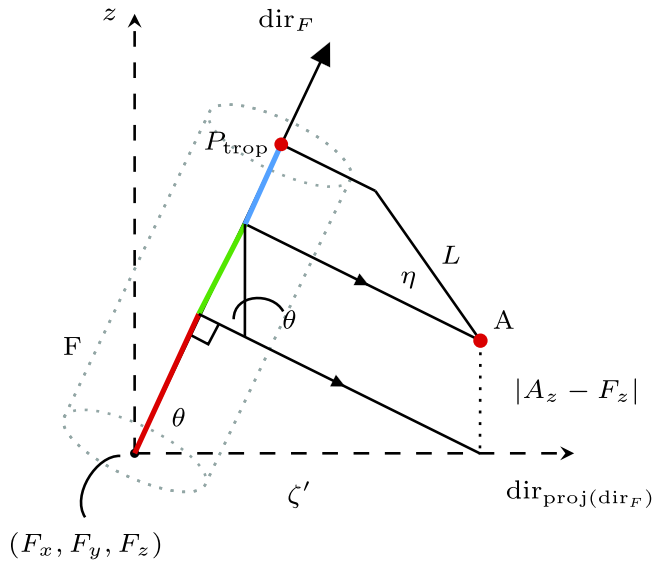

Fig. 3. When the apex A is too far from a climbing medium F, it grows towards F by use of a positional tropism. Interpretation of Eq. (5). Red = ζ' cos (θ); green = $|A_z - F_z|$ sin (θ); blue = L sin (η).

of the apex A, dir_F denotes the direction vector (head vector) of F, proj() is the projection to the (x, y)-plane, L is the length of the new internode, and η is the helix inclination. $|A_z - F_z|$ sin (θ) + ζ' cos (θ) represents the position on the pole for which the bean apex is in a plane perpendicular to the pole at this point. Rather than growing directly to this point, we envisage that bean plants would typically grow under a further inclination, and hence turn to grow towards a further point on the pole. We therefore introduce the additional term L sin (η), based on the inclination angle η (the steepness of the bean stem), which results in simulation outputs consistent with real-world observations.

2.2.2 Initial reorientation. At the start of a simulation, after a nonstandard turn (caused by either a tightening or a collision on the previous step) or when changing from one climbing medium to the next (e.g. when growing above a maize internode), assuming the apex is sufficiently close to the climbing medium, the apex must be reoriented to ensure it has the correct heading to continue on a helical trajectory. This is done using global-to-local and local-to-global transformation matrices (Fig. 4; Supplementary Material S1.2).

We start with an apex A and a climbing medium F, both with some arbitrary local coordinate system. Applying the local-to-global transformation matrix of A to this apex, transforms A's local coordinate system to the global coordinate system (e.g. A's left-, up-, and head-axes equal the global x-, y-, and z-axes, respectively). Subsequently, we apply the global-to-local transformation matrix of F to the apex A, which transforms A's local coordinate system to that of F (e.g. A's left-, up-, and head-axes equal F's respective local axes). A number of fixed local rotations are then applied to A to ensure the correct heading (see Supplementary Material S1.2 for more detail):

$$\text{RH}(\gamma)\ \text{RH}(\beta)\ \text{RL}(90^\circ)\ \text{RU}(\alpha)\ \text{RL}(\eta). \tag{6}$$

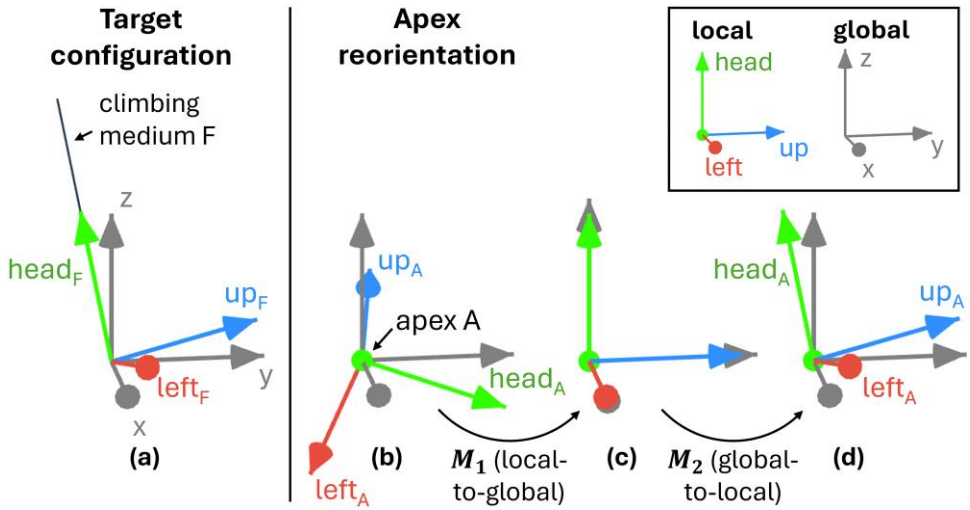

Fig. 4. Schematic showing the initial reorientation of a bean apex (b–d) given the orientation of the climbing medium (a) (see Section 2.2.2 for details). (a) local coordinate system of climbing medium F ((left, up, head)-axes in colour) and global coordinate system ((x, y, z)-axes in grey); (b) initial (arbitrary) local coordinate system of apex A; (c) transformation M_1 rotates A's local coordinate system to the global system; (d) subsequently applying transformation M_2 rotates A's local coordinate system to that of F.

Here, RH, RL, and RU are rotations around A's head-, left-, and up-axis, respectively. γ is the angle that rotates A's up-axis towards the centre of the pole F (Supplementary Fig. S6); $\beta = 90^\circ - \alpha/2$ is half of the inner polygon angle (Supplementary Fig. S7); α is the rotation angle on the current step (Section 2.2.3); and η is the inclination angle.

2.2.3 Rotation angle (normal, tightening, collision). The angle of the turn in the plane orthogonal to the climbing medium (α in Fig. 2 and Supplementary Fig. S7) is equal to

$$\alpha = 360^\circ/n, \tag{7}$$

where n is the number of sides of the polygon in F's (left,up)-plane (Supplementary Fig. S7). In our model, n is approximated by

$$n = \max\left(3, \left\lfloor \pi / \tan^{-1}\left(\frac{L\cos(\eta)}{2R}\right)\right\rceil\right), \tag{8}$$

yielding a polygon circumscribed to the circle with radius R. In the above, $\lfloor\cdot\rceil$ means rounding to the nearest integer. $L\cos(\eta)$ is the length of the projection of the new internode to the (left, up)-plane.

To initiate a turn, we first rotate down to the plane orthogonal to the climbing medium. Then, we turn with angle α (which for a normal turn equals $360^\circ/n$), and turn back up by an angle η to ensure the proper helix inclination:

$$\mathrm{RL}(-\eta)\ \mathrm{RU}(\alpha)\ \mathrm{RL}(\eta) \tag{9}$$

If a collision is detected under the current angle α, new angles are tried (from $\max(\alpha, 90^\circ)$ to -90° in steps of 1°) until an angle is found which does not lead to a collision. This new angle is then used instead of α (Fig. 2). In the next step, the transformations for reorienting the apex need to be applied (Section 2.2.2) as a different angle than α was used, which changes the helix centreline orientation.

Even if no collision is detected under the current angle α, it might be possible to increase this angle without resulting in a collision, leading to tighter (thus more realistic) coiling. To this end, at each step (assuming no collision was detected under angle α) an increased angle is tried (from $\alpha + 25^\circ$ to α° in increments of 1°). If the increased angle does not result in a collision, it is used instead of α. Again, in this case the transformations for reorienting the apex need to be applied in the next time step.

2.2.4 Collision detection. Collisions between the newly inserted bean internode and poles should be avoided, as they constitute nonphysical behaviour. Detecting cylinder–cylinder collisions is generally difficult (Supplementary Material 1.4). We therefore employ an approximate method, making use of GroIMP's capability of calculating line-volume intersections. Four lines are placed equidistant on the cylinder wall of the internode that is to be inserted under the new heading (characterized by the calculated angle α) (Supplementary Fig. S8), and intersections are calculated between these lines and any climbable object in the scene. If no intersections are detected, the internode is placed under this heading. If one or more intersections are detected, a new heading is tried as described in Section 2.2.3.

3. GLOBAL SENSITIVITY ANALYSIS (BEAN MONOCULTURE)

To gain insight into which parameters are most important in climbing bean development, and which parameters would thus merit further investigation in subsequent experiments, the elementary effects global sensitivity analysis (GSA) method (Rutjens et al. 2023) is applied to a monoculture of climbing bean growing on poles. GSA can in addition be used to investigate how important it is to improve the parameterization for bean, as this parameterization currently consists of values measured for common bean with different growth habits (e.g. bush bean), or values measured for climbing beans of a different

variety (i.e. not common bean), because data for climbing common bean were not available.

In earlier works, we modified the elementary effects method for dimensional models with inputs of arbitrary range and type (Rutjens et al. 2023), and for models with inherent randomness (Rutjens et al. 2024). The methodology as described in Rutjens et al. (2023, 2024) is therefore used here, e.g. using a radial trajectory design with $r = 20$ trajectories generated by the R_d quasi-random sequence. Both sensitivity indices S_χ (the median of absolute effects, nondimensionalized and normalized; Eq. (36) in Rutjens et al. 2023) and $S_{\mu^\star}$ (the mean of absolute effects, nondimensionalized and normalized; Eq. (35) in Rutjens et al. 2023) are computed, and the relative standard deviation of effects (Eq. (10) in Rutjens et al. 2024) is considered. An unimportance threshold of $h = 30\%$ is used (so the parameters with sensitivity indices (ranked from low to high) that sum to less than h are unimportant; see Eqs. (5) and (6) in Rutjens et al. 2024), and the importance threshold S_{0j} is set to $S_{0j} = 3\hat{\mu}_{0j}/2 + 3\hat{\sigma}_{0j}$ (so parameters with a sensitivity index higher than that value are important). Whenever the two sensitivity measures do not lead to significantly different classifications of important parameters, only results for S_χ are used. As in Rutjens et al. (2024), to deal with inherent model randomness, at each simulation point the average is taken over three replicates and effect outliers are systematically removed.

To keep the analysis computationally feasible, in this section, only the first 60 days of bean development are simulated. A field consists of 100 bean plants growing on poles, spaced 0.2 m within rows and 0.5 m between rows. Table 1 explains the 31 parameters that are varied, and lists their input ranges. Supplementary Table S4 lists all other relevant values that are kept fixed throughout the analysis.

Five outputs are the main focus in this analysis: LAI, (aboveground) biomass, accumulated CO_2, the fraction of incoming radiation that is absorbed by the canopy, and the average red/far-red light ratio in the canopy (average perceived by internodes). Some results for yield and harvest index are also shown, but since pod growth starts after Day 35 and only 60 days are simulated, and since we did not model pod filling in detail, biomass is a more informative output.

3.1 Results

Up to 7 out of 31 input parameters are classified as important for multiple outputs (Fig. 5, Table 1), most notably Parameter 4: LMA (leaf mass per area), Parameter 15: WmaxLeaf (theoretical maximal leaf mass) and Parameter 19: nitro (leaf nitrogen content). Furthermore, Parameter 27: tb (base temperature) is important for 3 outputs according to S_χ (2 for $S_{\mu^\star}$), Parameter 29: phyllochron is important for 3 (3 for $S_{\mu^\star}$), and Parameter 24: KNKL (ratio of leaf nitrogen and light extinction coefficients) is important for 2 (4 for $S_{\mu^\star}$). The newly introduced parameters to describe climbing bean are generally not among the most important parameters: Parameter 8: helixIncl (helix inclination) is only important for 2 outputs, Parameter 9: Lmax (maximal internode length) is only important for the fraction of radiation absorbed according to S_χ (and to canopy red/far-red ratio according to $S_{\mu^\star}$), and Parameter 10: branchConst (branching constant) is not important for any output.

Certain parameter combinations resulted in unrealistically large leaves (more than 20 cm width of the widest leaflet at the widest point; see Fig. 6A and C) (Lynch et al. 1991, Loko et al. 2018, Suárez et al. 2022). This indicates some parameter ranges may be incorrect or too large. In subsequent simulations (i.e. bean/maize polyculture and corresponding monoculture simulations) the model parameterization is therefore updated; see Supplementary Material Section S3.

Plots of the evolution of the outputs and corresponding sensitivity indices over time, of the relative standard deviation of effects, and of one-at-a-time (OAT) simulations for six example parameters with varying importance are available in Supplementary Material Section S3.

4. ASSESSING LIGHT CAPTURE IN MAIZE/BEAN POLYCULTURES AND RELATED MONOCULTURES

Having identified the important and unimportant parameters in the bean model for key outputs (e.g. LAI, biomass, assimilated CO_2), this section considers a stand of bean plants growing around maize. For the maize component, these polyculture simulations build on previous GSA of a maize model (including more species-independent parameters, such as those of the photosynthesis model) in Rutjens et al. (2024). We explore the effect of varying six bean parameters identified in Section 3 as important for several outputs, including one parameter specifically related to bean climbing (Table 2), whilst keeping the maize parameterization fixed. Three different environmental conditions are simulated, to assess the validity of the results across an environmental gradient.

4.1 Experimental design

One hundred bean/maize pairs are simulated on a 10-by-10 grid, with a row distance of 0.5 m and a plant distance of 0.2 m. The field is cloned 10 times in each direction to reduce border effects. Both bean and maize are simulated for at least 100 days of development. The total number of simulated days depends on the value of bean *germination delay*. This parameter determines how much later bean germinates than maize. This can be interpreted both as simultaneous planting followed by delayed germination, or delayed planting followed by equal germination time after planting. For simplicity, throughout this article, we talk about *germination delay* to cover both of these cases.

Four outputs are considered for each plant species separately, and for the total field: LAI (per unit land area), aboveground biomass (per unit land area), assimilated CO_2 (per unit land area) and fraction of radiation that is absorbed by the canopy.

For five bean germination delay values (7, 17, 27, 47, and 100 days after maize), six bean parameters are varied in a OAT design (based on results in Section 3.1) consisting of 11 uniformly spaced simulation points per parameter (Table 2).

A germination delay of 7 days is approximately the earliest possible germination date for bean; maize internodes (the climbing medium for bean) generally do not appear until that day with the used

Table 1. Bean parameters varied in Elementary Effects sensitivity analysis.

.	Parameter (source)	Description	Units	min_i	max_i	LAI[a]	Biom[b]	Yield	assCO$_2$[c]	fAbs[d]	fieldRFR[e]
1	**tav_a**	**Parameter for average daily temperature; see Eq. (2)**	**°C**	**21.33**	**26.07**	**5**	**x**	**2**	**x**	**x**	**x**
2	tav_b	Idem	°C	253.2465	309.5235	x	x	x	x	x	x
3	specificInternodeLength	Internode length per unit biomass (SIL)	m·g^{-1}	0.05	0.15	x	x	x	x	x	x
4	**LMA (Nassar et al. 2010, Zhang et al. 2020)**	**Leaf mass per unit area**	**mg·cm^{-2}**	**2.25**	**6.75**	**1**	**3**	**x**	**3**	**2**	**1**
5	leafAngleLower	Insertion angle of leafs with rank equal to or below rankLower	°	63	117	x	x	x	x	x	x
6	leafAngleUpper	Insertion angle of leafs with rank above rankLower	°	63	117	x	x	x	x	–	x
7	leafCurve	Leaf curvature - angle between bottom and top of leaf blade	°	21	39	x	x	x	x	x	x
8	**helixIncl**	**Helix inclination**	°	**35**	**75**	–	**x**	**x**	–	**4**	**2**
9	**Lmax**	**Maximal internode length**	**m**	**0.05**	**0.15**	**x**	**x**	**x**	**x**	**5**	–
10	branchConst	Constant ∈ [0, 1] that determines probability of branching	–	0.6	0.9	–	x	x	x	x	x
11	petioleFraction	Fraction of biomass partitioned to the petiole	–	0.0425	0.0575	x	x	x	x	x	x
12	wmaxRoot (Lynch and van Beem 1993, Beebe et al. 2006)	Maximal root system biomass (under ideal no-stress conditions)	mg	5000	15000	x	x	x	x	x	x
13	**wmaxFlower (Nassar et al. 2010)**	**Maximal flower biomass**	**mg**	**1000**	**3000**	–	**x**	**4**	**x**	**x**	**5**
14	wmaxInt (Nassar et al. 2010)	Maximal internode biomass	mg	150	450	x	x	x	x	x	x
15	**wmaxLeaf (Suárez et al. 2022)**	**Maximal leaf biomass**	**mg**	**1000**	**3000**	**3**	**5**	**x**	**4**	**1**	**4**
16	teRoot	Growth duration of root system (no growth after this time)	°C day	1620	1980	x	x	x	x	x	x
17	teFlower	Growth duration of flower	°C day	225	275	x	x	x	x	x	x
18	teLeaf	Growth duration of leaf	°C day	225	275	x	x	x	x	x	x
19	**nitro (Comstock and Ehleringer 1993)**	**Nitrogen content of fully lit leaf**	**g·m^{-2}**	**1**	**3**	–	**1**	**x**	**1**	–	**x**
20	leafLife	Life span of leaf since appearance (as multiple of teLeaf)	–	4	12	x	x	x	x	x	x
21	varDelay	Max variation in germination delay	day	0	3	x	x	x	x	x	x
22	seedMass (White and Montes-R 2005)	Seed endosperm mass	mg	150	600	x	-	x	x	x	x
23	rg (O'Callaghan et al. 1994)	Growth respiration	g·g^{-1} day^{-1}	0.289	0.391	x	–	x	x	x	x
24	**kNkL**	**Ratio of leaf nitrogen and light extinction coefficients (k_N/k_L)**	–	**0.2**	**1**	**x**	**2**	**x**	**2**	**x**	**x**
25	rm (O'Callaghan et al. 1994)	Maintenance respiration	g·g^{-1} day^{-1}	0.01445	0.01955	x	x	x	x	x	x
26	**fCO2**	**Conversion factor of CO_2 to biomass**	–	**0.51**	**0.69**	**x**	**4**	**x**	**x**	**x**	**x**
27	**tb (Nleya et al. 2005)**	**Base temperature for thermal time calculation**	**°C**	**8**	**14**	**6**	**x**	**3**	**x**	**x**	**7**
28	plastochronconst	Plastochron (thermal time between creation of two phytomers) is this constant (∈ [0, 1]) times phyllochron, to ensure that plastochron is smaller than phyllochron	–	0.8	0.95	x	x	x	x	x	x

(*continued*)

Table 1. Continued

.	Parameter (source)	Description	Units	min_i	max_i	LAI[a]	Biom[b]	Yield	$assCO_2^c$	fAbs[d]	fieldRFR[e]
29	phyllochron (Ricaurte et al. 2016)	Thermal time between appearance of two leaves	°C day	50	75	4	x	x	5	3	–
30	finalPhytNum	Final number of main stem vegetative phytomers	–	4	14	x	–	1	x	x	3
31	fallPAR	Light level below which leaf drops	μmol $m^{-2}s^{-1}$	20	100	2	x	x	x	x	6

All parameters are real numbers except 21 ($p_{21} = 4$, $|\delta_{21}| = 2/3$) and 30 ($p_{30} = 6$, $|\delta_{30}| = 3/5$), which are integers. The right-most columns indicate whether a parameter is unimportant (x), important (**bold**; number indicates rank, 1 being most important) or neither (-) for six outputs at simulation Day 60. [a]: peak leaf area index; [b]: peak aboveground biomass; [c]: peak assimilated CO_2; [d]: peak fraction of radiation absorbed; [e]: canopy red/far-red ratio at final simulation day. For parameters that were kept fixed in the analysis, see Supplementary Material 6.1.

maize parameters (Fig. 7). All maize parameters are fixed, see Supplementary Material S5 for a full list of parameter values. As a further means of comparison, bean and maize are simulated in monoculture (bean in the OAT design listed in Table 2 with a germination delay of 27 days; see Supplementary Material S5.2 for baseline values). Furthermore, it is investigated how plant development changes in a different climatic environment, by simulating bean and maize both in monoculture and in polyculture in three sets of environmental conditions (e.g. temperature, transmissivity of the sky, day length, and position of the sun): Mexican (Yucatán region), France (Aquitaine region) and the Netherlands. Dutch environmental conditions were chosen for three reasons: (i) maize is commonly grown in the Netherlands for animal fodder; (ii) maize/bean polycultures have been grown in very similar environmental conditions (e.g. in northern Germany Fischer et al. 2020, Austria Böhm et al. 2022 and North-East Switzerland Carrel Strickhof); and (iii) detailed environmental data for the Netherlands was readily available in the model. The Aquitaine region in the south-west of France was further included to serve as an intermediate between the more extreme Mexican and Dutch environments: the latitude and temperature profile lie between the Dutch and Mexican values. In this region, maize and some bean species are also grown (Béasse and Kouassi 2019). For transmissivity of a clear sky in the Aquitaine region, no values were found in the literature, so a value in between the Mexican and Dutch values was chosen (SupplementaryTable S7).

4.2 Results

4.2.1 Local sensitivity analysis for key bean parameters. In general, maize exhibits a very minor response to the presence of bean, regardless of the chosen bean input parameter values; even if bean is planted as soon as the first maize internodes emerge (see Fig. 8 for peak LAI and a bean germination delay of 27 days and Supplementary Figs. S29–S31; first column for other outputs and delays), changes in maize LAI due to aboveground competition are small (peak maize LAI only varies between 1.2 and 1.5). Maize peak output values respond most strongly to a change in bean leaf mass per area when maize and bean germinate in quick succession (Supplementary Figs. S29–S31; third row, first column), but even then changes in maize peak values are relatively small compared to bean (maize peak LAI varies between 1.2 and 1.5, whereas bean peak LAI varies between 0 and 3.8 for varying LMA).

In OAT simulations of the polyculture under Mexican environmental conditions, bean base temperature is least impactful of the 6 parameters considered, followed by phyllochron and helix inclination. For all environmental conditions, outputs are more sensitive to changes in leaf nitrogen content and the theoretical maximal leaf weight, and leaf mass per area is clearly the most influential parameter (see Fig. 8 for peak LAI and a bean germination delay of 27 days, and Supplementary Figs. S29–S31 and S35–S36 for other outputs, delays and environments).

4.2.2 Monoculture versus polyculture. Maize output values for the monoculture and polyculture are extremely similar [Fig. 8 for peak LAI values with a bean planting delay of 27 days; and Supplementary Figs. S29–S31 for results with different planting delays and outputs (compare green and black lines)]. This is not surprising, as maize barely responded to the presence of common bean. Bean on the other hand shows significant changes between monoculture and polyculture, performing much worse in the polyculture than in a monoculture (Fig. 8). In most cases (in Mexican conditions), the polyculture outperforms the maize monoculture, in the sense that the total peak LAI (see Fig. 8 for a bean germination delay of 27 days, and Supplementary Fig. S32 for other delay values), aboveground biomass (Supplementary Fig. S33) and assimilated CO_2 (Supplementary Fig. S34) over 100 days of maize and bean development is higher than the highest peak maize values over all simulations.

4.2.3 Effect of bean germination delay. The following is based on results for Mexican environmental conditions only, as bean performed poorly under French and Dutch conditions (further discussed in Section 4.2.4), and focuses on three outputs: LAI, biom (aboveground biomass) and fAbs (fraction of radiation absorbed by leaves). The maximum maize LAI (during the first 100 days of development) hardly depends on the value of the bean germination delay (Fig. 9 lower panel). For bean, output values typically decrease with an increase in bean germination delay up to some point, but outputs increase for longer delays (Fig. 9 lower panel). This complex dependence of peak bean output values (during 100 days of development) on bean germination delay can be understood by considering five possible phases in which bean could be planted (Figs. 9 and 10). Figure 9 (top panel) shows the maize LAI varies during the growing season, with maize LAI increasing during the first 40 days (Phases I–III), plateauing during the next 40 days (Phase IV) and then reducing during the final 30 days (Phase V). The phase (I–V) in which the bean is

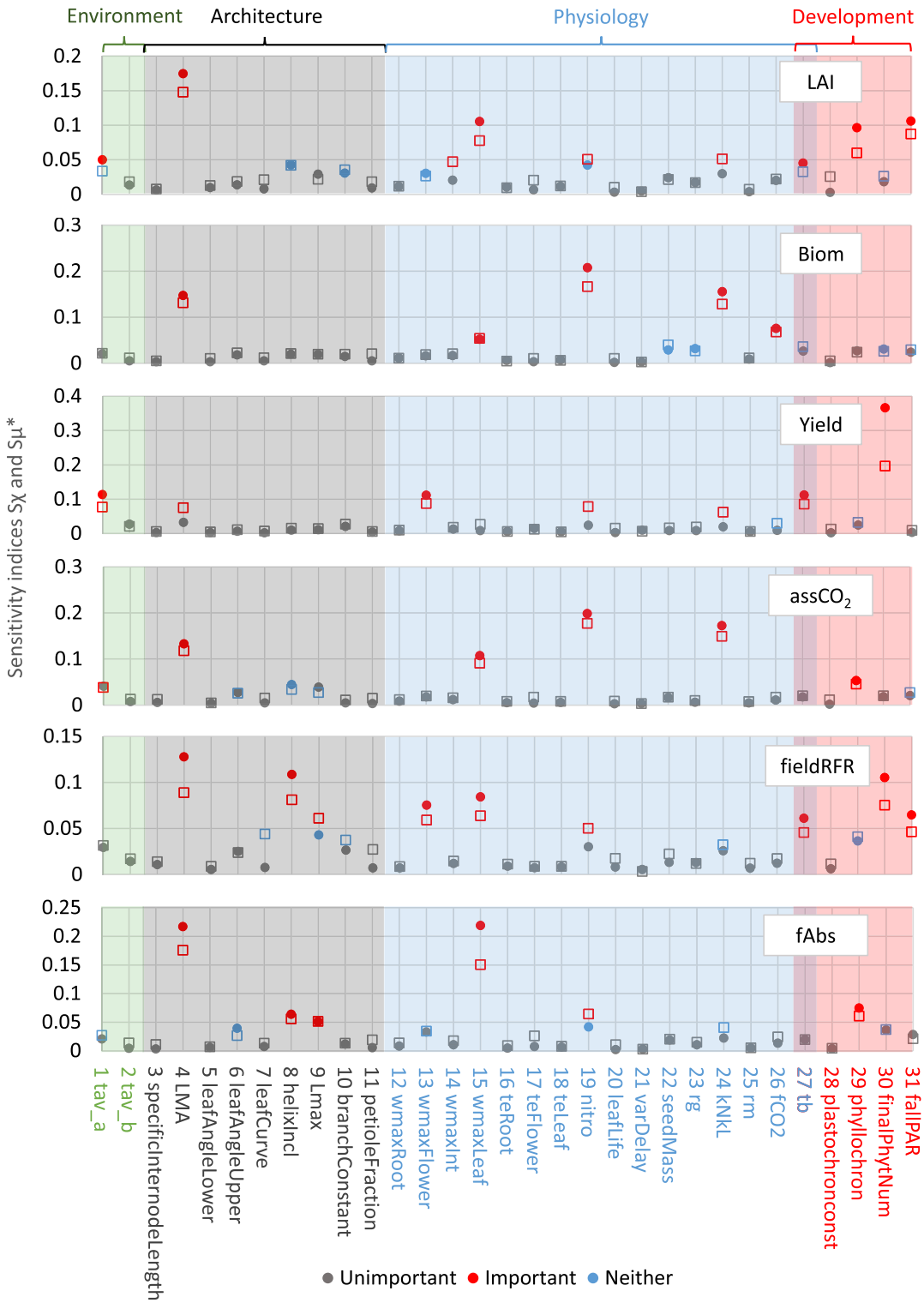

Fig. 5. Global sensitivity of a monoculture of common bean climbing on poles under Mexican environmental conditions. Sensitivity indices for several field-level outputs at peak value (LAI, aboveground biomass (biom), yield, assimilated CO_2 ($assCO_2$), fraction of radiation absorbed (fAbs)) or final value (canopy red/far-red ratio (fieldRFR)). Circles: S_χ; squares: $S_{\mu^\star}$.

planted determines the behaviour of the peak bean LAI, fAbs, and biom values (bottom panel). In the first phase (bean delay between 7 and 21 days), the peak LAI, fAbs and biom values for bean decrease with germination delay, whilst there is an increase in peak maize LAI. In the second phase (21–30 days delay), bean peak LAI, fAbs and biom values remain approximately constant, even though maize LAI increases linearly (over time). Phase III (30–45 days) seems to be a transition phase for bean peak values from constant to increasing. In Phase IV (45–70 days) a linear increase in peak bean output

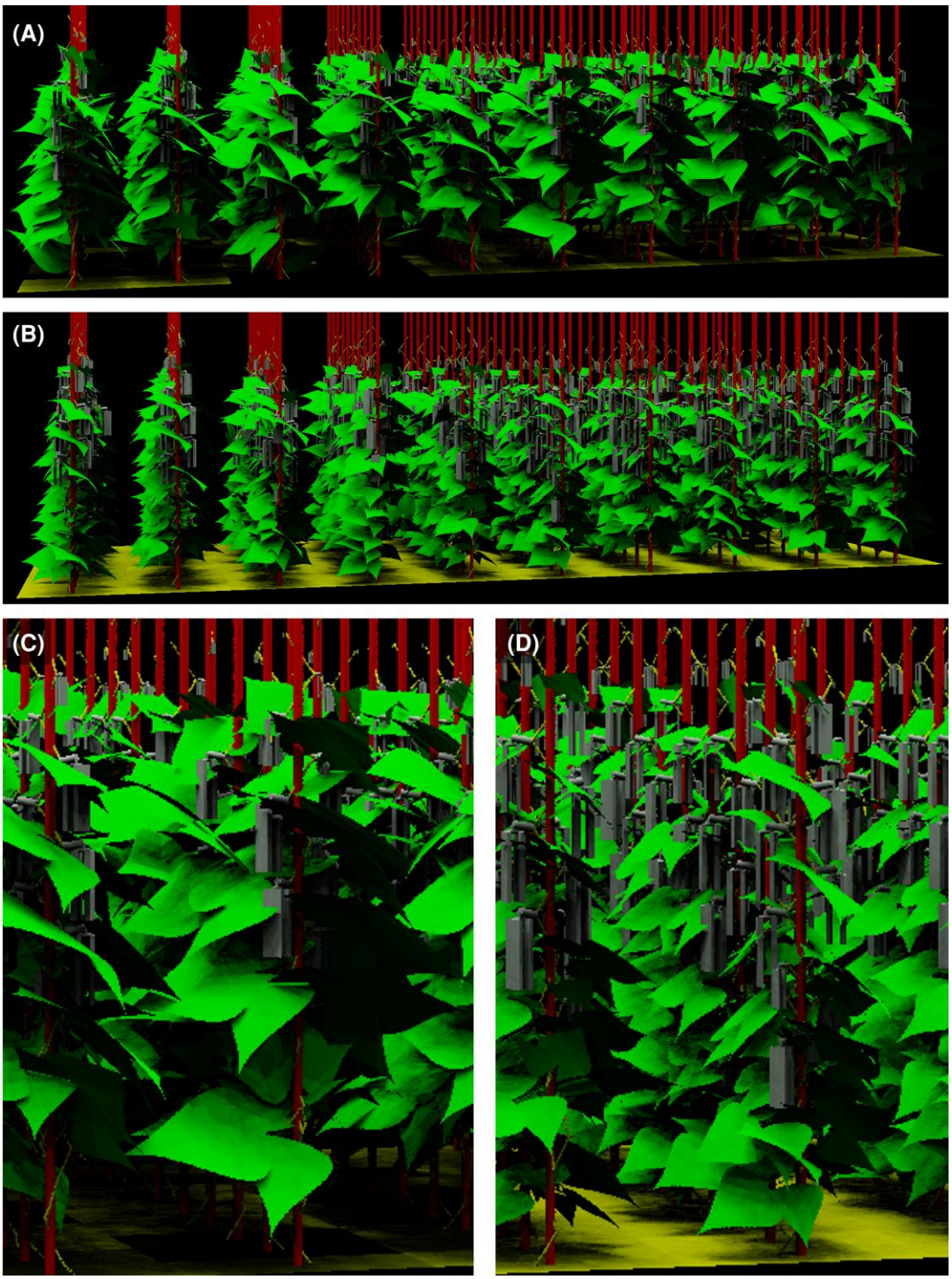

Fig. 6. Architectural differences in a stand of common bean caused by a difference in leaf mass per area (LMA; parameter 4) (which is deemed an important parameter for all outputs except yield) at the end of simulation day 60. The other parameters are set to the mean of their input ranges (Supplementary Table S3). (a) LMA = 2.25 g/m^2; lower bound of input range. LAI = 6.5, aboveground biomass = 1,577 g/m^2, yield = 154 g/m^2, assimilated CO_2 = 2.1 mol/m^2, fraction of radiation absorbed = 0.73, canopy red/far-red ratio = 0.44. (b) LMA = 6.75 g/m^2; upper bound of input range. LAI = 3.4, aboveground biomass = 646 g/m^2, yield =149 g/m^2, assimilated CO_2 = 1.6 mol/m^2, fraction of radiation absorbed = 0.57, canopy red/far-red ratio = 0.52. (c) Close-up of (a). (d) Close-up of (b).

values is observed, which accelerates in the last phase (70–100 days). Over the whole time period, temperature and day length do not vary as much as maize LAI, and are thus unlikely to dominate bean output values (Supplementary Fig. S38). The biological interpretation of these observations is discussed in Section 5.2.2.

Table 2. Polyculture simulations: six bean parameters are varied in a OAT design, consisting of 11 uniformly spaced simulation points per parameter.

Parameter	Meaning	Unit	Min.	Max.
WmaxLeaf	Maximal leaf mass	mg	200	2000
nitro	Leaf nitrogen content	$g{\cdot}m^{-2}$	1	3
LMA	Leaf mass per area	mg/cm^2	3	8
tb	Base temperature	°C	8	14
phyllochron	Phyllochron	°C days	50	75
helixIncl	Helix inclination	°	35	75

4.2.4 Effect of environmental conditions. Both maize and common bean development are significantly affected by the environmental conditions, both in a polyculture (see Fig. 11 for peak LAI, and Supplementary Figs. S35 and S36 for other outputs) and in their respective monocultures (Figs. 12 and 13). In the monoculture, both maize and bean assimilate less CO_2 in French conditions compared to Mexican conditions, and even less in Dutch conditions, and produce less biomass as a result, most likely due to lower temperatures and less incoming radiation (Fig. 13). This effect is more severe for bean (80% less biomass under Dutch conditions compared to Mexican conditions at the final simulation day) than for maize (55% less) (Fig. 13). Leaf area production in maize starts slower in French conditions and Dutch conditions, and peak LAI is higher than in Mexican conditions (Fig. 13). For bean, LAI follows a similar trend to CO_2 assimilation, producing much less leaf area in French conditions, and even less in Dutch environmental conditions (Figs. 12 and 13). The same holds for the polyculture (with a bean germination delay of 27 days): maize peak LAI increases from ∼1.4 (Mexican conditions) to just under 2 (Dutch conditions) (Fig. 11), maize peak aboveground biomass drops from 1.2 to under 0.5 kg/m^2, and maize assimilated CO_2 drops from ∼1.3 to ∼0.6 mol/m^2 (Supplementary Fig. S36). Bean performs poorly in the polycultures in French and Dutch conditions, with all peak output values barely above zero for almost all combinations of input parameters (see Fig. 11 for peak LAI, and Supplementary Figs. S35 and S36 for other outputs).

The baseline value for bean base temperature in the OAT simulations is 11°C. The same OAT simulations were also run for French environmental conditions and a lower bean base temperature of 8°C to confirm whether the lower performance (compared to Mexican conditions) was due to lower average temperatures, but the output values were mostly indistinguishable from the ones under the higher base temperature; they are therefore not shown here.

5. DISCUSSION

This study aimed to test the hypothesis: *architectural facilitation in the bean/maize polyculture leads to enhanced light capture (hence improved biomass production) when compared to growing these crops in monoculture*. By creating an FSP model for climbing common bean, we were able to simulate such polycultures, and confirm that for most parameter values tested, and in the right environment, the hypothesis was true (see Section 5.2.4 for details). Additionally, our results provided further insights, both from a modelling and biological perspective, which are detailed below.

5.1 Modelling insights

GSA for bean model. There is considerable uncertainty in a number of bean parameter values, for example because the only values found in the literature were for common bean with a determinate growth habit or for climbing plants of a different variety, or because no data were available in the literature. Relatively wide parameter ranges were therefore chosen for such parameters. If such a parameter is nevertheless identified as unimportant, it means it is also unimportant in a subrange. However, if it is classified as important, this might be due to the wide input range instead (the elementary effects might only be large for parameter values close to the extremes of the input range), suggesting it would be instructive to refine the input range first, before concluding the parameter itself is important. This is for example the case for Parameter 15: WmaxLeaf (theoretical maximum leaf weight), which was identified as important for most outputs, but whose input range was found to be too wide upon revisiting the literature (see Supplementary Material S3).

5.1.2 Bean internode initiation. Under French and Dutch environmental conditions, a lack of growth in common bean was observed (compared to Mexican conditions). Whilst this is undoubtedly partly due to the environmental parameters themselves (lower average temperature, less incoming radiation), these results may have been exacerbated by the modelling choice to initiate bean internodes with their final length (recall: to prevent 'loosening' of the helix over time). In the real world, maize and bean internodes elongate over time, but in the model this is only implemented for maize. This means that the initial resource cost for initiating a bean internode and maintenance costs directly after initiation are higher than what they would be if bean internode elongation would have been implemented. Consequently, there are less resources available for bean leaf growth directly after appearance of an internode, and thus these smaller leaves will not be able to capture as much light. This effect then propagates and grows over time, potentially leading to underestimation of assimilated CO_2 (and hence LAI and aboveground biomass) by bean.

5.1.3 Decomposing internode into sub-internodes. It has been reported that final internode lengths for climbing bean can reach 10–15 cm (and in extreme cases even more than 20 cm) (Davis et al. 1984, Checa and Blair 2008, González et al. 2021), while the diameter of the pole is typically just a few centimetres. Approximating a continuous helix by a discrete one with such long internodes might therefore lead to a poor representation of the climbing bean plant, with the leaves (situated at the internode end points) emerging relatively far from the pole. Therefore, it could be important to decompose the bean internodes into a number of smaller sub-internodes. This can improve visual realism and, more importantly, potentially increase model accuracy. We therefore extended the model to include sub-internodes. The full derivation and results can

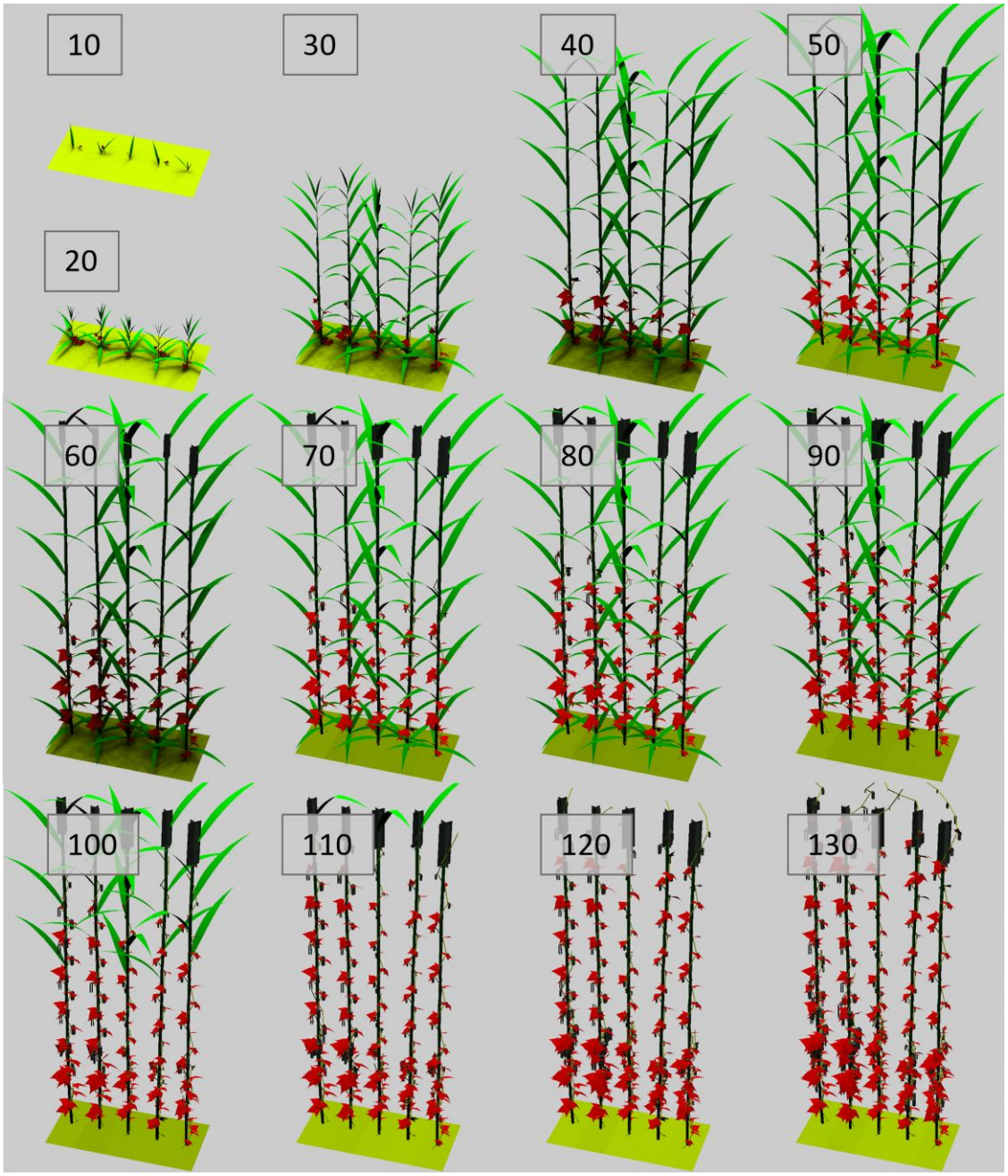

Fig. 7. Illustrative example of 3D output over time, taking a snapshot (front view) of the scene every 10 days. Green: maize leaves; red: common bean leaves. Bean germination delay is 7 days. Day of snapshot is indicated in text boxes.

be found in Supplementary Material S2. We found that, for a subset of the GSA and OAT parameter explorations presented above, the impact on the main (nonvisual) model outputs was very small, but computational cost and model complexity increased significantly; we therefore did not use sub-internodes in this work.

5.1.4 Weather data. In this work, simple daily mean temperature profiles based on climate data from the past decades were used to create three distinct environmental scenarios. Other atmospheric parameters, such as CO_2 level, vapour pressure deficit and O_2 level were kept fixed and equal across environments. Since the purpose of this plant modelling study was to investigate the intricate relations between plant traits and performance for an architecturally complex system, this coarser approach was justified. If the purpose instead would have been to e.g. make yield predictions for such systems, considering the full suite of atmospheric parameters, using accurate short-term weather data, and taking variation from the climatic average into account would be crucial. This would also open interesting avenues for further research, for example, using such models together with future weather predictions to assess agricultural production potential in different geographical regions.

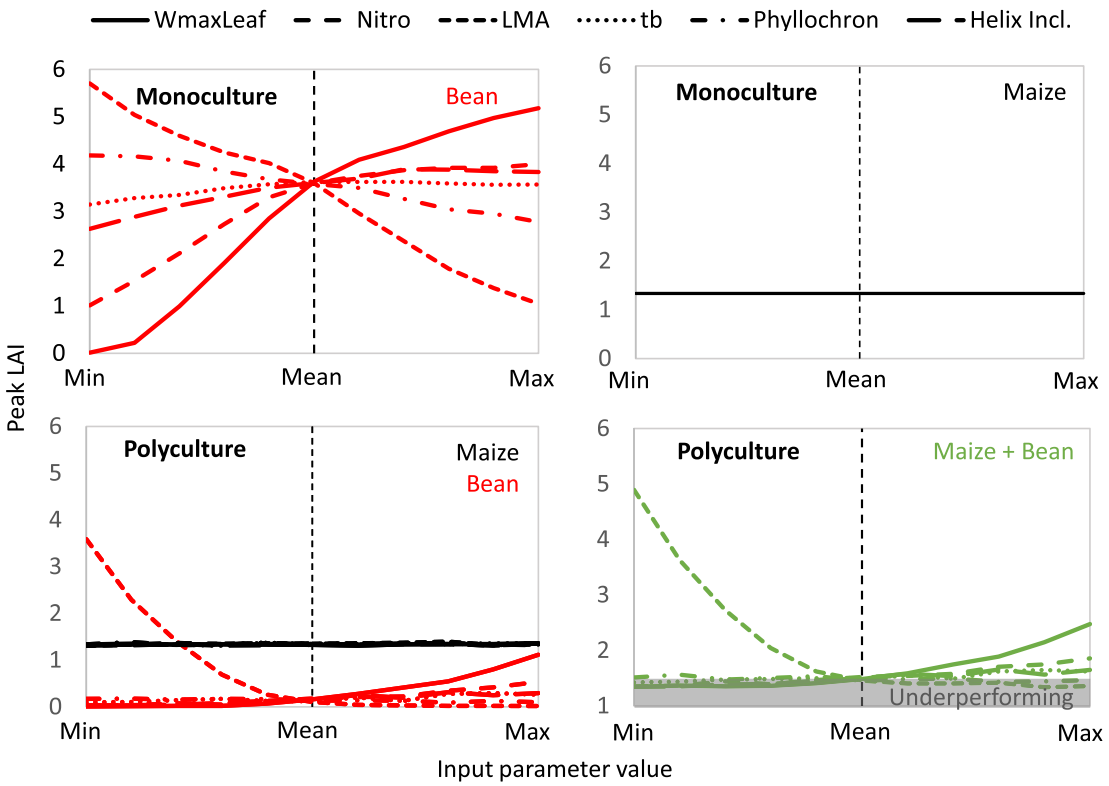

Fig. 8. Monoculture versus polyculture: peak LAI during 100 days of development for each crop in a bean and maize monoculture (top) and maize/bean polyculture (bottom), varying six bean input parameters. Mexican environmental conditions, 27 days bean germination delay. Black: maize; red: common bean; green: total (sum of peak values for bean and maize). Grey highlighted area indicates *underperforming* in the polyculture w.r.t. the highest maize value (incl. maize monoculture). Vertical lines indicate OAT baseline. These results show that LMA and WmaxLeaf are the most important input parameters.

5.2 Biological insights

5.2.1 Effect of bean parameters in polyculture simulations. Leaf mass per area (LMA) and the theoretical maximal leaf weight (WmaxLeaf) were found to be the most influential parameters in the OAT simulations. Compared to the baseline value, peak bean LAI increased as much as 20-fold for the lowest LMA value, and six-fold for the highest value of WmaxLeaf. These increases in peak LAI cannot be explained by an increase in leaf size alone, as leaf width increased from its baseline value by a factor <1.5 (Supplementary Fig. S37; left panel). Considering LMA, a significant increase in bean branching (3.5 times baseline value) was observed for the lowest LMA value (Supplementary Fig. S37; right panel), in combination with a moderate leaf size increase (average leaf width: 1.5 times baseline value). The lower the value for LMA, the 'cheaper' it is to produce new leaf tissue. More resources can then be allocated to other organs, such as internodes, leading to increased branching. This in turn results in more leaves (as only one leaf can emerge from a single internode). Nevertheless, this still does not fully explain the increase in leaf area which would only be $\sim 1.5^2 \cdot 1.4 \cdot 3.5 \approx 11$ times the base value (length increase is width increase times length/width ratio (=1.4)). For WmaxLeaf, there is no noticeable increase in branching and thus in the number of leaves (Supplementary Fig. S37; right panel): as leaves are not 'cheaper' to produce (as was the case with LMA), there is no surplus of resources with a higher WmaxLeaf value. The only difference is that more resources may be allocated to a leaf, leading to an increased surface area of that leaf. Again, the increase in average leaf size (average leaf width: 1.2 times baseline value) only explains approximately a $1.2^2 \cdot 1.4 \cdot 1 \approx 2$-fold increase in LAI with larger WmaxLeaf. As such, the increase in peak LAI can be partially explained by these calculations. However, the discrepancy between these calculated values and model predictions suggests that the dynamics also have a major influence, with larger leaves capturing more light, and thus generating more resources for growth at subsequent time steps, in a self-amplifying manner.

Maize is hardly affected by bean, likely because it typically outgrows bean from the start (Fig. 7 provides a front view, Supplementary Fig. S39 a top-down view), so only the bottom few leaves experience shading from the bean (depending on the bean germination delay). By the time bean reaches the top of the maize plant, in most cases all maize leaves have dropped (Fig. 7). Since that is the only competition we modelled, this results in a very minor negative effect on maize light capture. This agrees broadly with experimental findings by Clark and Francis (1985b), who wrote: 'in climbing bean intercrops, half to two-thirds of the maize leaf area was located above 150 cm, when averaged over the bean pod filling interval. Differences in bush and climbing bean leaf area display were apparent only in [...] the bottom and middle strata'.

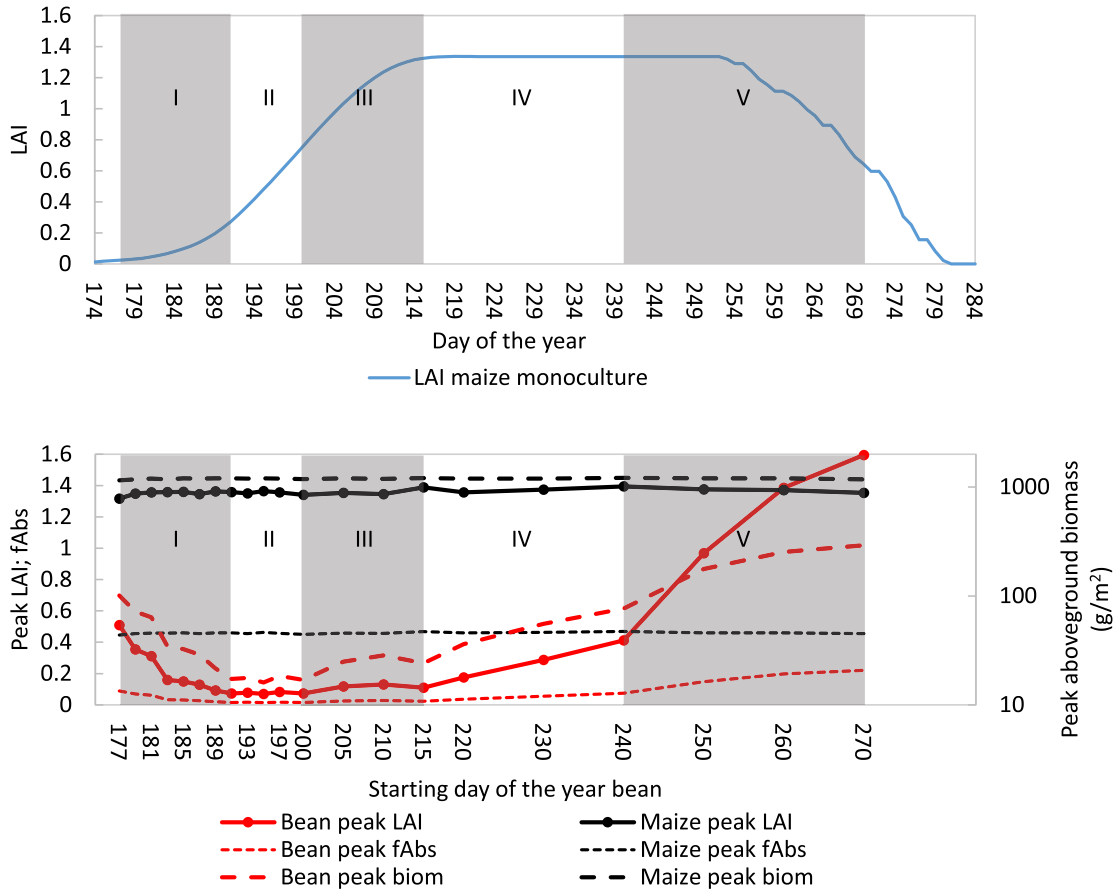

Fig. 9. The effect of bean germination delay on model outputs. Top: maize LAI over time. Bottom: peak LAI, fraction of radiation absorbed (fAbs) and aboveground biomass (biom) for bean and maize at different bean delay values (7–100 days); the horizontal axis denotes the starting day of the year for bean germination, assuming Maize planting occurred at Day 170. The regions I–V distinguish different behaviour of the peak values (bottom), and are related to maize LAI at the day bean is planted (top). See also Fig. 10.

5.2.2 Effect of bean germination delay. Recall that the effect of bean germination delay on peak bean values over 100 days of development can be divided into five distinct time periods (Figs. 9 and 10). Phase I shows exponential propagation of early competition by shading: although maize LAI is low throughout this phase, a small increase in maize LAI at the day of emergence of bean leads to a significant decrease in bean performance, leading to a much more pronounced decrease of peak bean outputs. See also Nurk et al. (2017), who observed a similar decrease in biomass during field experiments in Germany (but for larger delay values), and Francis et al. (1982), who performed field trials with varying (but lower) relative bean germination delays in Colombia. This decrease in bean performance holds to some point (indicated by the transition of Phase I into Phase II), where bean apparently experiences maximal shading; bean peak values become nearly constant in this phase, even though maize LAI is still increasing. The additional maize leaf area at bean emergence apparently does not contribute to additional shading of the bean plant. This behaviour continues in Phase III, where maize attains a fully grown canopy. In Phases IV and V, bean is already experiencing the maximum amount of shading at emergence. From that point onward, it is beneficial to emerge even later (although the day length and temperature, and thus thermal time accumulation, drop slightly), as bean then spends less time growing under a full maize canopy, and receives more light once maize leaves are shed. Since the bottom maize leaves shed first, the opposite effect to that in Zone I is visible: a decline in maize LAI at bean emergence leads to an increase in bean peak values. The sharp change in steepness of the bean peak curves on the interface of Phase IV and V is likely smooth in practice, and caused by the sparsity of sample points in that region. At the end of Phase V, the bean peak curves flatten; at this point, the overlap (in time) between maize and bean becomes so small (it takes typically <10 days from that point onward before maize sheds its final leaf), so that the peak bean values only depend on accumulated thermal time, which varies much more slowly.

5.2.3 Effect of environmental conditions. Differences in simulated maize development under Dutch environmental conditions compared to the Yucatán peninsula (Figs. 11 and 13) can be explained as follows. The slower onset of leaf area, and the lower peak values of assimilated CO_2 and aboveground biomass are caused by a decrease in incoming radiation, and lower temperatures and less hours of daylight, leading to less thermal time accumulation. Higher peak LAI under Dutch

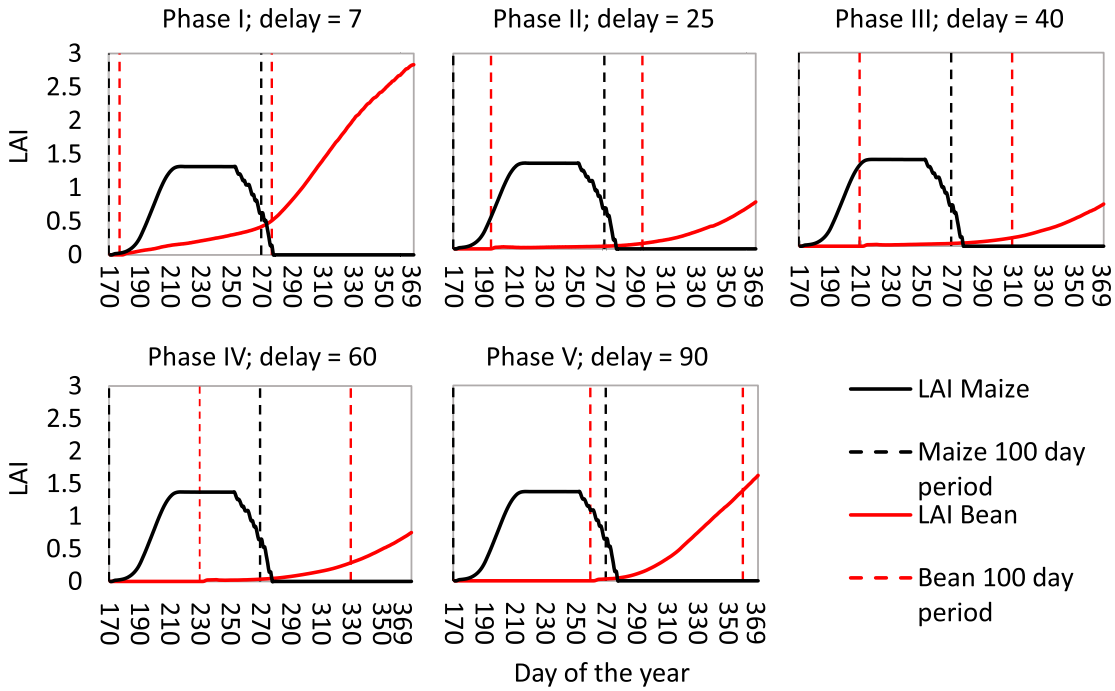

Fig. 10. The effect of bean germination delay on model outputs. LAI over time for five delay values shown in Fig. 9 (bottom). Each of the panels corresponds to a different phase (I–V) in Fig. 9. Dashed lines mark the start and end of the first 100 days of development. Maize leaves start to senesce from around Day 250.

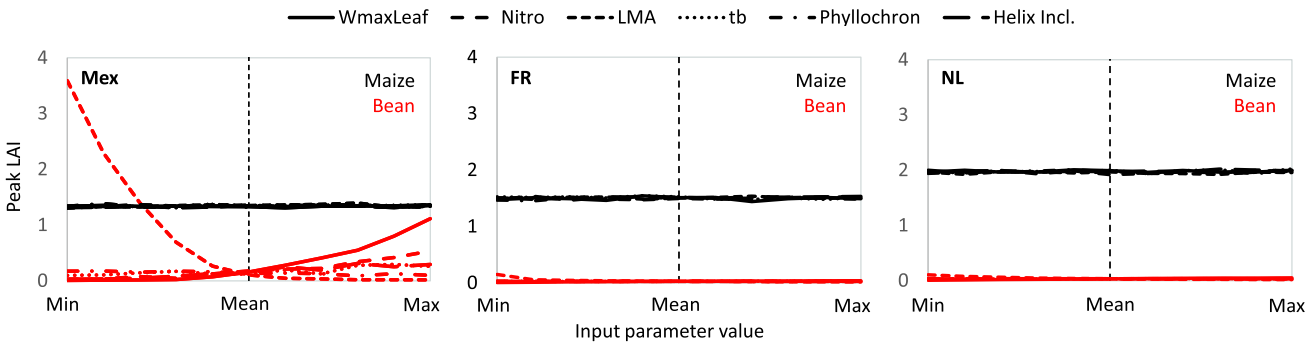

Fig. 11. Effect of environment: peak LAI during 100 days of development for each crop in a maize/bean polyculture, varying six input parameters. Mex: Mexico (Yucatán), FR: France (Aquitaine), NL: Netherlands. Black: maize; red: common bean. Vertical lines indicate OAT baseline. In all panels, bean germination was delayed by 27 days. Common bean barely developed in French and Dutch conditions.

conditions can be attributed to a change in resource allocation ratios to the different organs. Under Dutch conditions the maize shoot/root biomass ratio (ratio of leaf plus stem mass and root mass at the day peak LAI was reached) was six times higher than under Mexican conditions (based on simulation results; not shown here), suggesting that although the total plant biomass was lower, there were still more resources allocated to the stem and leaves than in the Mexican case. Plant height was found to be roughly equal in both environments (based on simulation results; not shown here), indicating that the number of leaves was equal in each case, hence the individual leaves were larger under Dutch conditions. This means that under Dutch conditions, leaves got closer to their theoretical maximal weight. The same explanation holds for the differences between Mexican and French, and French and Dutch environments, but to a lesser degree.

5.2.4 Monoculture versus polyculture. Pleasant and Burt (2010) found in experiments (New York, USA) that maize yields were not affected by the presence of bean (and squash) in a three sisters polyculture, yielding as well in the polyculture as in monoculture. However, bean (and squash) yields were greatly reduced when grown with maize compared to in monoculture. This is further confirmed in field trials by e.g. Francis (1982) (Colombia) and in observations reported by Gliessman (2014) (Mesoamerica). Francis (1982) found that

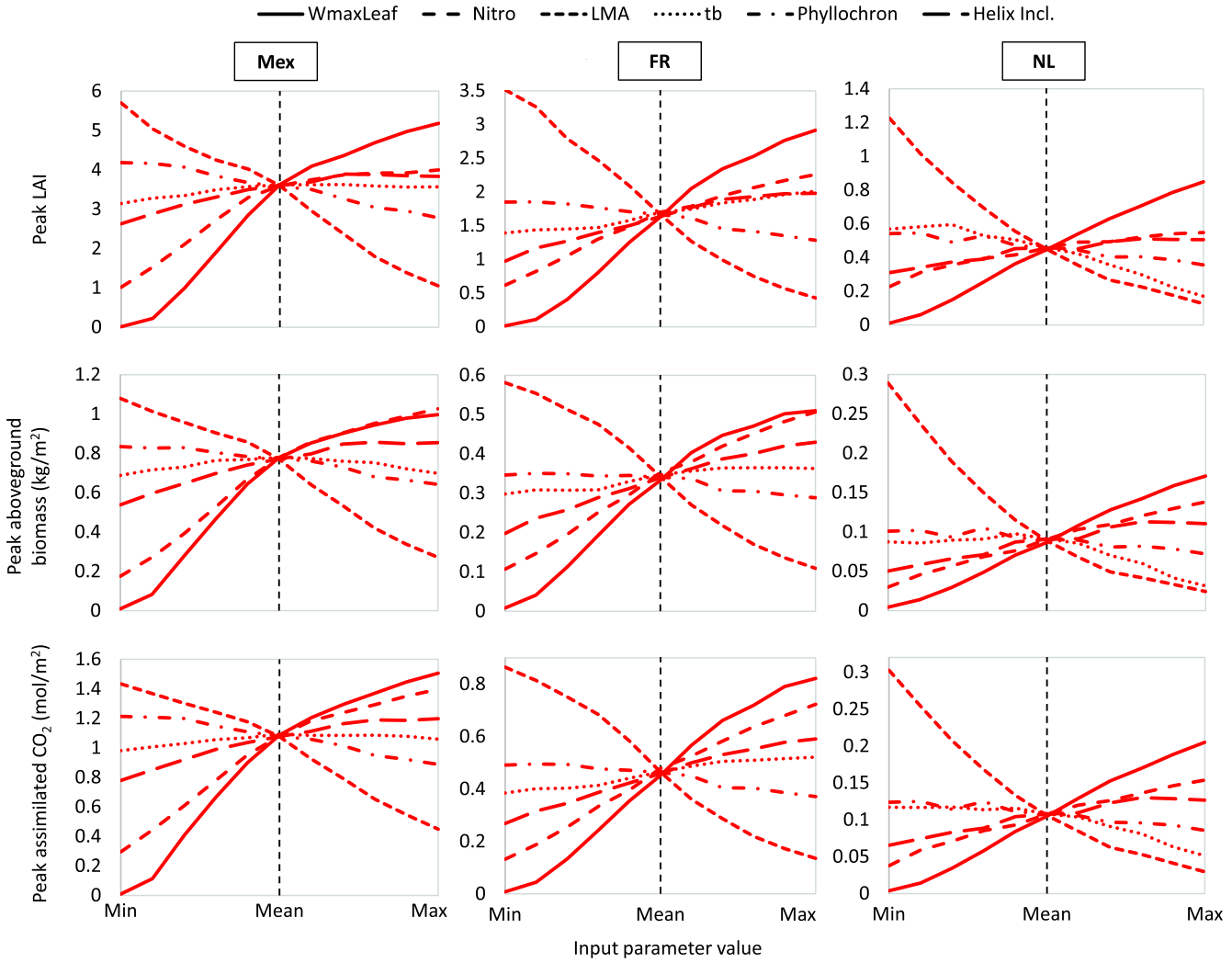

Fig. 12. Effect of environment: one-at-a-time variation of six parameters for simulations of a common bean monoculture growing on poles in different environmental conditions (Mex: Mexico (Yucatán), FR: France (Aquitaine), NL: Netherlands). Bean germination delay is 27 days. Note the different scales on the vertical axes.

'maize yield generally was unaffected by the undersown beans, but that the beans produced only 25–50% of their monocrop yield potential at comparable bean densities' (Clark and Francis 1985a). Moreover, Gliessman (2014) states that maize/bean(/squash) polycultures typically yield higher than the corresponding monocultures, although bean and squash yield significantly lower in a polyculture. Our simulation results (Fig. 8 for peak LAI and a bean germination delay of 27 days, Supplementary Figs. S32–S34 for other outputs and delays) are consistent with these findings for maize and bean, showing overperforming in combined LAI (up to 350% increase compared to peak maize values), aboveground biomass (up to 60% increase) and CO_2 assimilation (up to 85% increase, likely leading to overyielding) in Mexican environmental conditions for a variety of input parameter combinations and all bean germination delay values. Additionally, maize was hardly affected by the presence of bean, whilst bean performance was significantly reduced in polyculture (e.g. under Mexican conditions and with average parameter values, peak LAI decreased by 80% compared to the monoculture).

5.2.5 Limitations. This discussion provides some model validation through qualitative comparisons with existing data (Francis 1982, Francis et al. 1982, Clark and Francis 1985a, 1985b, Pleasant and Burt 2010, Gliessman 2014, Nurk et al. 2017). However, the results here were not quantitatively validated against real-world observations, because suitable data were not available in the literature (as evidenced by the difficulty encountered in the parameterization of climbing bean). To fully validate the model and the results presented here, detailed experimental studies of bean/maize polycultures (and potentially of the respective monocultures) are required, where extensive crop parameter data is recorded (with a focus on FSP model data requirements) alongside field-level outputs such as LAI and yield. We hope our study may motivate such studies in the future, and may stimulate more detailed observational data of climbing common bean.

In light of the uncertainty in the parameterization of common bean, it is also worth highlighting the importance of the biological limits imposed by genetic variation available in a population and potential trade-offs between plant traits.

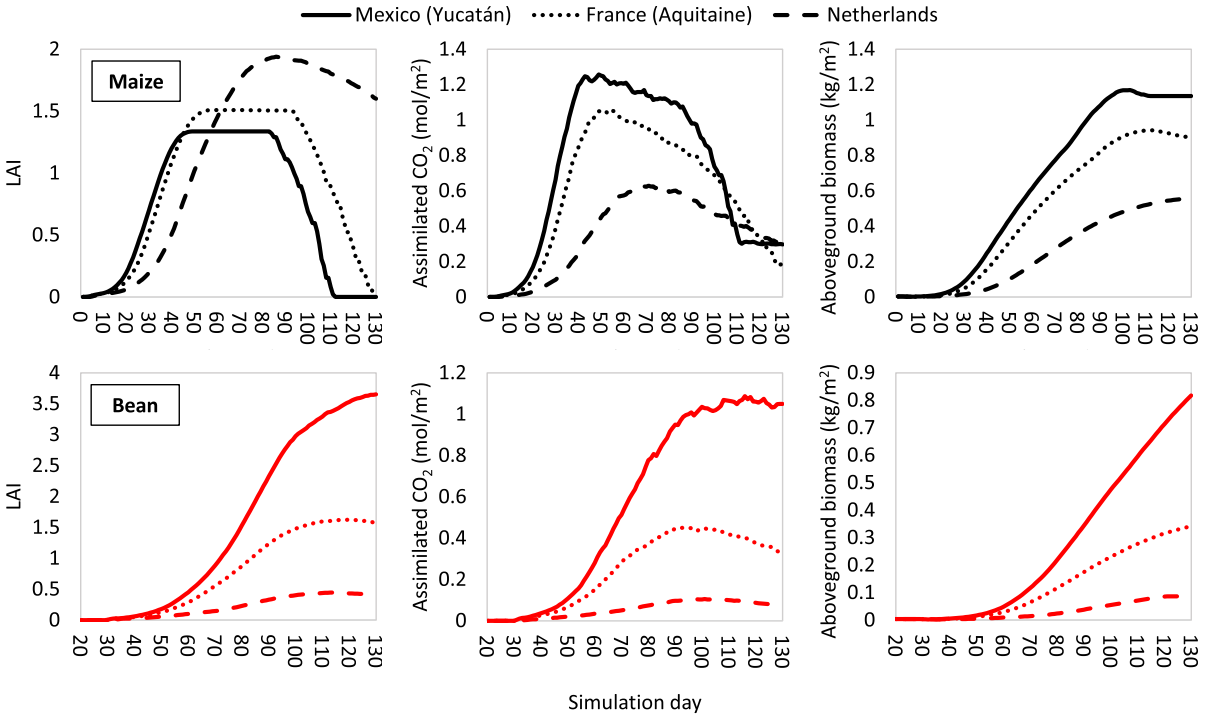

Fig. 13. Effect of environment: three field-level outputs over time for a monoculture of maize (black) and bean (red) in different environments: Mexico (Yucatán region), France (Aquitaine) and the Netherlands. Parameter values are given in Supplementary Material S5.2.

Varying plant parameters beyond what is currently observable in the population can be relevant: to identify how to obtain theoretical overyielding, or in breeding for modifying plant architecture. However, when the aim is to e.g. quantify yield potential in a certain environment, plant traits should be constrained to those that could occur in a population.

6. CONCLUSION

In this work, an FSP model for climbing common bean was presented. As far as we are aware, this is the first aboveground FSP of a climbing bean.

Our results generally agreed with reports in the literature of overyielding in polycultures including maize and climbing bean. Our simulations showed overperforming in LAI, aboveground biomass and CO_2 assimilation (likely leading to overyielding) in Mexican environmental conditions for a variety of input parameter combinations, and all bean germination delay values (Fig. 8 for peak LAI and a bean germination delay of 27 days, Supplementary Figs. S32–S34 for other outputs and delays). Maize was typically hardly affected by the presence of bean, whilst bean was sensitive to the presence of another crop. Thus, even though the model used here did not include plant root architecture and heat or water stress, key characteristics of this polyculture were still recovered. This indicates that aboveground processes (also) play an important role in the phenomenon of overperformance (overyielding).

From a farm management perspective, our simulations indicate it is best to have bean germinate either as early as possible (e.g. as soon as maize stems are sufficiently established, but while maize leaves are still small and few), or very late (e.g. when maize leaves start to senesce), effectively turning the polyculture into a sequence of two monocultures.

Environmental conditions had a significant effect on model outputs, most notably on the behaviour of common bean. For our model, Bean grew best in Mexican conditions, and hardly grew in South-French or Dutch conditions (Fig. 11). While our results are naturally affected by model assumptions and parameterization, they indicate that maize/bean polycultures are most beneficial in environments with higher average temperatures and incoming radiation.

We conclude from this first proof of principle of an FSP polyculture model with complex plant–plant interaction that FSP modelling is a valuable tool to investigate such agricultural systems. With this work, we have shown that it is possible to model maize/bean polycultures, paving the way for models of even more complex systems (e.g. the three sisters or milpa).

ACKNOWLEDGEMENTS

This work was supported by the University of Nottingham Future Food Beacon of Excellence.

SUPPLEMENTARY DATA

Supplementary data is available at *in silico Plants* online.

Conflict of interests: None declared.

FUNDING

None declared.

DATA AVAILABILITY

The numerical results were obtained using code in the RGG language (Kniemeyer 2008) (an extension of Java), compiled on the freely available modelling environment GroIMP (Hemmerling et al. 2008). Included in the code is a stand-alone implementation of our formulation of EE. The data—including additional figures—are available in the form of Microsoft Excel spreadsheets. Code and data that support the findings of this study are openly available at https://github.com/pmxrr3/maizebeanpolyculture_2023 and as supplementary materials to this article.

REFERENCES

Altieri MA. The ecological role of biodiversity in agroecosystems. *Invertebrate Biodiversity as Bioindicators of Sustainable Landscapes* 1999;**74**:19–31. https://doi.org/10.1016/B978-0-444-50019-9.50005-4

Altieri MA, Nicholls CI. Agroecology and the reconstruction of a post-COVID-19 agriculture. *J Peasant Stud* 2020;**47**:881–898. https://doi.org/10.1080/03066150.2020.1782891

Arvo J, Kirk D. Modeling plants with environment-sensitive automata. In: *Proceedings of Ausgraph'88*. Citeseer.

Atala C, Gianoli E. Induced twining in *Convolvulaceae* climbing plants in response to leaf damage. *Botany* 2008;**86**:595–602. https://doi.org/10.1139/B08-037

Bahr C, Schmidt D, Friedel M *et al.* Leaf removal effects on light absorption in virtual Riesling canopies (*Vitis vinifera*). *In Silico Plants* 2021;**3**:diab027. https://doi.org/10.1093/insilicoplants/diab027

Barillot R, Escobar-Gutiérrez AJ, Fournier C *et al.* Assessing the effects of architectural variations on light partitioning within virtual Wheat–Pea mixtures. *Ann Bot* 2014;**114**:725–737. https://doi.org/10.1093/aob/mcu099

Béasse C, Kouassi AS. Characterization of the weed flora in open field vegetable systems in the sandy area of the moors (New Aquitaine). Alfortville, France: Végéphyl—Association pour la santé des végétaux, 2019.

Beebe SE, Rojas-Pierce M, Yan X *et al.* Quantitative trait loci for root architecture traits correlated with phosphorus acquisition in common bean. *Crop Sci* 2006;**46**:413–423. https://doi.org/10.2135/cropsci2005.0226

Benes B, Míllán EU. Virtual climbing plants competing for space. In: *Proceedings of Computer Animation 2002 (CA 2002)*. 33–42. IEEE, 2002.

Böhm H, Aulrich K, Baldinger L *et al.* Maize intercropped with climbing beans: from cultivation to feeding. 2022. https://www.legumehub.eu/wp-content/uploads/2022/02/Maize-intercropped-with-climbing-beans-en.pdf. Accessed 20 August 2023.

Carrel (Strickhof) K. Aktuelles zum Anbau von Mais-Bohnen-Mischkulturen. 2020. https://www.strickhof.ch/publikationen/aktuelles-zum-anbau-von-mais-bohnen-mischkulturen/. Accessed 20 August 2023.

Checa OE, Blair MW. Mapping QTL for climbing ability and component traits in common bean (*Phaseolus vulgaris L.*). *Mol Breed* 2008;**22**:201–215. https://doi.org/10.1007/s11032-008-9167-5

Clark EA, Francis CA. Bean-maize intercrops: a comparison of bush and climbing bean growth habits. *Field Crops Res* 1985a;**10**:151–166. https://doi.org/10.1016/0378-4290(85)90023-1

Clark EA, Francis CA. Transgressive yielding in bean:maize intercrops; interference in time and space. *Field Crops Res* 1985b;**11**:37–53. https://doi.org/10.1016/0378-4290(85)90090-5

Comstock J, Ehleringer J. Stomatal response to humidity in common bean (*Phaseolus vulgaris*): implications for maximum transpiration rate, water-use efficiency and productivity. *Funct Plant Biol* 1993;**20**:669–691. https://doi.org/10.1071/PP9930669

Davis JHC, Van Beuningen L, Ortiz MV *et al.* Effect of growth habit of beans on tolerance to competition from maize when intercropped. *Crop Sci* 1984;**24**:cropsci1984.0011183X002400040029x. https://doi.org/10.2135/cropsci1984.0011183X002400040029x

Dubois JJB, Fiscus EL, Booker FL *et al.* Optimizing the statistical estimation of the parameters of the Farquhar–von Caemmerer–Berry model of photosynthesis. *New Phytologist* 2007;**176**:402–414. https://doi.org/10.1111/nph.2007.176.issue-2

Durigon A, Evers J, Metselaar K *et al.* Water stress permanently alters shoot architecture in common bean plants. *Agronomy* 2019;**9**:160. https://doi.org/10.3390/agronomy9030160

Evers JB, Bastiaans L. Quantifying the effect of crop spatial arrangement on weed suppression using functional-structural plant modelling. *J Plant Res* 2016;**129**:339–351. https://doi.org/10.1007/s10265-016-0807-2

Fiorello I, Del Dottore E, Tramacere F *et al.* Taking inspiration from climbing plants: methodologies and benchmarks—a review. *Bioinspir Biomim* 2020;**15**:031001. https://doi.org/10.1088/1748-3190/ab7416

Fischer J, Böhm H, Heß J. Maize-bean intercropping yields in Northern Germany are comparable to those of pure silage maize. *Eur J Agron* 2020;**112**:125947. https://doi.org/10.1016/j.eja.2019.125947

Francis CA. Density interactions in tropical intercropping. I. Maize (*Zea mays* L.) and climbing beans (*Phaseolus vulgaris* L.). *Field Crops Res* 1982;**5**:163–176. https://doi.org/10.1016/0378-4290(82)90016-8

Francis CA, Prager M, Tejada G. Effects of relative planting dates in bean (*Phaseolus vulgaris* L.) and maize (*Zea mays* L.) intercropping patterns. *Field Crops Res* 1982;**5**:45–54. https://doi.org/10.1016/0378-4290(82)90005-3

Gliessman SR. *Agroecology: The Ecology of Sustainable Food Systems*, 3rd edn. Boca Raton: CRC Press, 2014.

González AM, Yuste-Lisbona FJ, Weller J *et al.* Characterization of QTL and environmental interactions controlling flowering time in andean common bean (*Phaseolus vulgaris* L.)). *Front Plant Sci* 2021;**11**:599462. https://doi.org/10.3389/fpls.2020.599462

Goriely A, Neukirch S. Mechanics of climbing and attachment in twining plants. *Phys Rev Lett* 2006;**97**:184302. https://doi.org/10.1103/PhysRevLett.97.184302

Goudriaan J, Van Laar HH. *Modelling potential crop growth processes*. **Vol. 2**. Dordrecht: Kluwer Academic Publishers, 1994.

Greene N. Voxel space automata: modeling with stochastic growth processes in voxel space. *SIGGRAPH Comput Graph* 1989;**23**:175–184. https://doi.org/10.1145/74334.74351

Hädrich T, Benes B, Deussen O *et al.* Interactive modeling and authoring of climbing plants. *Comput Graph Forum* 2017;**36**:49–61. https://doi.org/10.1111/cgf.2017.36.issue-2

Hemmerling R, Kniemeyer O, Lanwert D *et al.* The rule-based language XL and the modelling environment GroIMP illustrated with simulated tree competition. *Funct Plant Biol* 2008;**35**:9–10. https://doi.org/10.1071/FP08052

Heuvelink E. Re-interpretation of an experiment on the role of assimilated transport resistance in partitioning in tomato. *Ann Bot* 1996;**78**:467–470. https://doi.org/10.1006/anbo.1996.0143

Huber M, Nieuwendijk NM, Pantazopoulou CK *et al.* Light signalling shapes plant–plant interactions in dense canopies. *Plant Cell Environ* 2021;**44**:1014–1029. https://doi.org/10.1111/pce.v44.4

Isnard S, Cobb AR, Holbrook NM *et al.* Tensioning the helix: a mechanism for force generation in twining plants. *Proc R Soc Lond B Biol Sci* 2009;**276**:2643–2650. https://doi.org/10.1098/rspb.2009.0380

Kahlen K, Stützel H. Modelling photo-modulated internode elongation in growing glasshouse cucumber canopies. *New Phytol* 2011;**190**:697–708. https://doi.org/10.1111/nph.2011.190.issue-3

Kelly JD. Remaking bean plant architecture for efficient production. *Adv Agron*. 2001;**71**:109–143. https://doi.org/10.1016/S0065-2113(01)71013-9

Kniemeyer O. Design and implementation of a graph grammar based language for functional-structural plant modelling. Doctoral Thesis, 2008.

Knutzen J. Generating climbing plants using L-systems. Doctoral Thesis, Chalmers university of technology Göteborg, Sweden, 2009.

Li S, van Der Werf W, Zhu J *et al.* Estimating the contribution of plant traits to light partitioning in simultaneous maize/soybean intercropping. *J Exp Bot* 2021;**72**:3630–3646. https://doi.org/10.1093/jxb/erab077

Loko LEY, Orobiyi A, Adjatin A *et al.* Morphological characterization of common bean (*Phaseolus vulgaris* L.) landraces of Central region of Benin Republic. *J Plant Breed Crop Sci* 2018;**10**:304–318. https://doi.org/10.5897/JPBCS

López-Forment IS. Changes in diversity in the process of milpa intensification in the Henequen zone in Yucatán, Mexico. In: *1998 Meeting of the Latin American Studies Association*. Chicago, Illinois, 1998, 24–26.

Lynch J, Läuchli A, Epstein E. Vegetative growth of the common bean in response to phosphorus nutrition. *Crop Sci* 1991;**31**: cropsci1991.0011183X003100020031x. https://doi.org/10.2135/cropsci1991.0011183X003100020031x

Lynch J, van Beem JJ. Growth and architecture of seedling roots of common bean genotypes. *Crop Science* 1993;**33**:1253–1257. https://doi.org/10.2135/cropsci1993.0011183X003300060028x

Maya Forest Gardeners - The Milpa. https://mayaforestgardeners.org. Accessed 13 July 2023.

Moulton DE, Oliveri H, Goriely A. Multiscale integration of environmental stimuli in plant tropism produces complex behaviors. *Proc Natl Acad Sci U S A* 2020;**117**:32226–32237. https://doi.org/10.1073/pnas.2016025117

Météo-France. Average monthly temperatures for the Aquitaine region of France (1991–2020). https://meteofrance.com/climat/normales/france/nouvelle-aquitaine. Accessed June 2025.

Nassar RM, Ahmed YM, Boghdady MS. Botanical studies on *Phaseolus vulgaris* L. I - morphology of vegetative and reproductive growth. *Int J Bot* 2010;**6**:323–333. https://doi.org/10.3923/ijb.2010.323.333

Nleya T, Ball RA, Vandenberg A. Germination of common bean under constant and alternating cool temperatures. *Can J Plant Sci* 2005;**85**: 577–585. https://doi.org/10.4141/P04-151

Nurk L, Graß R, Pekrun C *et al.* Effect of sowing method and weed control on the performance of maize (*Zea mays* L.) intercropped with climbing beans (*Phaseolus vulgaris* L.). *Agriculture* 2017;**7**:51. https://doi.org/10.3390/agriculture7070051

O'Callaghan JR, Maende C, Wyseure GCL. Modelling the intercropping of maize and beans in Kenya. *Comput Electron Agric* 1994;**11**: 351–365. https://doi.org/10.1016/0168-1699(94)90026-4

Pleasant JM. Food yields and nutrient analyses of the three sisters: a haudenosaunee cropping system. *Ethnobiol Lett* 2016;**7**:87–98. https://doi.org/10.14237/ebl.7.1.2016

Pleasant JM, Burt RF. Estimating productivity of traditional Iroquoian cropping systems from field experiments and historical literature. *J Ethnobiol* 2010;**30**:52–79. https://doi.org/10.2993/0278-0771-30.1.52

Postma JA, Lynch JP. Complementarity in root architecture for nutrient uptake in ancient maize/bean and maize/bean/squash polycultures. *Ann Bot* 2012;**110**:521–534. https://doi.org/10.1093/aob/mcs082

Ricaurte J, Clavijo Michelangeli JA, Sinclair TR *et al.* Sowing density effect on common bean leaf area development. *Crop Sci* 2016;**56**: 2713–2721. https://doi.org/10.2135/cropsci2016.01.0056

Rutjens RJL, Band LR, Jones MD *et al.* Elementary effects for models with dimensional inputs of arbitrary type and range: scaling and trajectory generation. *PLoS One* 2023;**18**:e0293344. https://doi.org/10.1371/journal.pone.0293344

Rutjens RJL, Evers JB, Band LR *et al.* Are we focusing on the right parameters? Insights from global sensitivity analysis of a functional-structural plant model. *In Silico Plants* 2024;**6**:diae011. https://doi.org/10.1093/insilicoplants/diae011

Schmook B, van Vliet N, Radel C *et al.* Persistence of Swidden cultivation in the face of globalization: a case study from communities in Calakmul, Mexico. *Hum Ecol* 2013;**41**:93–107. https://doi.org/10.1007/s10745-012-9557-5

Sievänen R, Godin C, DeJong TM *et al.* Functional–structural plant models: a growing paradigm for plant studies. *Ann Bot* 2014;**114**: 599–603. https://doi.org/10.1093/aob/mcu175

Smolenova K, Hemmerling R. Growing virtual plants for virtual worlds. In: *Proceedings of the 24th Spring Conference on Computer Graphics*, Association for Computing Machinery, Budmerice Castle, Slovakia, 2008. https://doi.org/10.1145/1921264.1921280.

Spitters CJT. Separating the diffuse and direct component of global radiation and its implications for modeling canopy photosynthesis part II. Calculation of canopy photosynthesis. *Agric For Meteorol* 1986;**38**: 231–242. https://doi.org/10.1016/0168-1923(86)90061-4

Spitters CJT, Toussaint HAJM, Goudriaan J. Separating the diffuse and direct component of global radiation and its implications for modeling canopy photosynthesis part I. Components of incoming radiation. *Agric For Meteorol* 1986;**38**:217–229. https://doi.org/10.1016/0168-1923(86)90060-2

Suárez JC, Casanoves F, Di Rienzo J. Non-destructive estimation of the leaf weight and leaf area in common bean. *Agronomy* 2022;**12**:711. https://doi.org/10.3390/agronomy12030711

Tilman D, Reich PB, Knops J *et al.* Diversity and productivity in a long-term grassland experiment. *Science* 2001;**294**:843–845. https://doi.org/10.1126/science.1060391

Tsubo M, Mukhala E, Ogindo HO *et al.* Productivity of maize-bean intercropping in a semi-arid region of South Africa. *Water SA* 2003;**29**:381–388. https://doi.org/10.4314/wsa.v29i4.5038

White JW, Montes-R C. Variation in parameters related to leaf thickness in common bean (*Phaseolus vulgaris* L.). *Field Crops Res* 2005;**91**: 7–21. https://doi.org/10.1016/j.fcr.2004.05.001

Wong S-K, Chen K-C. A procedural approach to modelling virtual climbing plants with tendrils. *Comput Graph Forum* 2016;**35**:5–18. https://doi.org/10.1111/cgf.2016.35.issue-8

World Bank. Average monthly temperatures for Yucatán (1991–2020; based on data by the Climatic Research Unit of University of East Anglia). https://climateknowledgeportal.worldbank.org/country/mexico/climate-data-historical. Accessed June 2025.

Yin X, Goudriaan JAN, Lantinga EA *et al.* A flexible sigmoid function of determinate growth. *Ann Bot* 2003;**91**:361–371. https://doi.org/10.1093/aob/mcg029

Yin X, Struik PC. C3 and C4 photosynthesis models: an overview from the perspective of crop modelling. *NJAS - Wageningen J Life Sci* 2009;**57**:27–38. https://doi.org/10.1016/j.njas.2009.07.001

Zhang M, Zhang S, Ye M *et al.* The genetic control of leaf allometry in the common bean, *Phaseolus vulgaris*. *BMC Genet* 2020;**21**:29. https://doi.org/10.1186/s12863-020-00838-2